ORNL/TM--9361

DE85 004768

ENVIRONMENTAL SCIENCES DIVISION

MINERALOGICAL CHARACTERIZATION OF WEST CHESTNUT RIDGE SOILS

S. Y. Lee, O. C. Kopp[1], and D. A. Lietzke[2]

Environmental Sciences Division
Publication No. 2418

NUCLEAR AND CHEMICAL WASTE PROGRAMS
(Activity No. AR 05 10 05 K; ONL-WL13)

Date Published - December 1984

---

[1]Department of Geological Sciences, University of Tennessee, Knoxville, TN 37916

[2]Department of Plant and Soil Science, University of Tennessee, Knoxville, TN 37916

Prepared for the
Office of Defense Waste and Byproducts Management

Prepared by the
OAK RIDGE NATIONAL LABORATORY
Oak Ridge, Tennessee 37831
operated by
MARTIN MARIETTA ENERGY SYSTEMS, INC.
for the
U.S. DEPARTMENT OF ENERGY
under Contract No. DE-AC05-840R21400

TABLE OF CONTENTS

LIST OF FIGURES

LIST OF TABLES

ACKNOWLEDGMENTS

The authors wish to acknowledge the assistance of H. C. Monger, Jr., who conducted the soil survey of the site, and P. D. Lowry and A. L. Thomas, who provided excellent technical support. We thank J. Switek and R. H. Ketelle for their suggestions and technical reviews of this report, and B. J. Cochran for secretarial assistance in the preparation of this report.

ABSTRACT

LEE, S. Y., O. C. KOPP, and D. A. LIETZKE. 1984. Mineralogical characterization of West Chestnut Ridge soils. ORNL/TM-9361. Oak Ridge National Laboratory, Oak Ridge, Tennessee. 94 pp.

The morphological, physicochemical, and mineralogical properties of the soils and residua from the proposed site of the Central Waste Disposal Facility were characterized. The proposed site, which is located in the West Chestnut Ridge area of Roane County, Tennessee, is underlain by cherty dolostones, limestones, and shales of the Knox Group covered by a thick residuum. The pedogenic soil horizons developed from ancient and younger alluvium, colluvium, and residuum. The soils are classified into nine mapping units; most are variants of the Fullerton, Etowah, Shack, Dewey, and Holston series of the Paleudult great group, which developed on the freely drained, very old, and stable land surfaces in humid climates.

Three diagnostic horizons from four soil profiles and six samples from residuum cores were selected for mineralogical analysis. The coarse fractions (gravel and sand) of the samples included different types of chert, iron-manganese oxide nodules, and quartz.

The samples were high in clay content (except those from the A and E horizons) and low in pH and base saturation. The clay fractions were composed of varying amounts of kaolinite, mica, vermiculite, aluminum hydroxy-interlayered vermiculite, amorphous iron and aluminum oxides, gibbsite, and quartz. Aluminum hydroxy-interlayered vermiculite is the major component in surface horizons, but kaolinite becomes dominant in subsurface horizons of the soils. Degradation of kaolinite and

formation of aluminum hydroxy-interlayered vermiculite and iron and aluminum oxides are pronounced chemical weathering processes in the surface soils. The aluminum hydroxy interlayering of vermiculite reduces cation exchange and selective sorption capacities of soils.

In the residua, micaceous minerals free of aluminum hydroxy interlayering, kaolinite, and amorphous iron and aluminum oxides are major components in the clay fraction. The sorption ratios of ^{137}Cs, ^{90}Sr, ^{60}Co, and the uranium isotopes expected to be in the radioactive wastes should be very high for the clays having such mineralogical composition. The low acid-buffering capacity (base saturation) of the residua suggest that the fragile chemical and mineralogical equilibria can be easily broken if an extreme chemical condition is imposed on the residua. Therefore, the existing favorable physicochemical and mineralogical conditions for radionuclide retardation in the residua can be maintained only through proper waste disposal practices.

INTRODUCTION

A section of West Chestnut Ridge in Roane County, Tennessee, has been selected as a candidate site for a new low-level radioactive waste disposal facility (designated the Central Waste Disposal Facility) for the Department of Energy's Oak Ridge plants. The significant factors considered during the selection processes were bedrock geology, surface and subsurface hydrology, physicochemical properties of the soil, geographic setting, long-term structural stability, and management of the site after waste disposal and closure (Lee et al. 1983a).

At the selected site, the Knox Group is composed mostly of dolostones, with some limestones, shales, and sandstones, and is covered by up to 30 m of residuum, colluvium, and alluvium. The residuum is composed of chert, quartz, and clay minerals, which may in some places have been redistributed by alluvial and eolian processes. The soils developed in an environment of moderately warm temperatures (2-24°C), comparatively high annual rainfall (120 cm), and forest cover, but the soils differ widely in morphology, texture, reaction, and degree of stoniness and erosion.

Soils and underlying geomedia often act as a purifying filter for water containing dissolved and colloidal materials. Radionuclide retardation is governed primarily by the physical and chemical properties of the soil minerals. Dominant clay minerals in the dolostone residuum were anticipated to be kaolinite, micaceous minerals, iron and aluminum oxides, and quartz (Carroll 1961). Each mineral has different physicochemical characteristics, which affect the bulk physical, chemical, hydrologic, and structural properties of the

soil and residuum. This report contains a small-scale soil survey map of West Chestnut Ridge and information on soil morphology, and the physical, chemical, and mineralogical properties of the soil profiles. Physicochemical and mineralogical properties of selected residuum samples from the proposed site are also presented.

Knowledge of pedogenesis, geochemical processes, and mineral distribution should help in the prediction of radionuclide migration or accumulation and the management of land and vegetation after closure of the site.

SITE DESCRIPTION

GEOLOGY

The proposed site is located in the Whiteoak Mountain thrust sheet, one of several subparallel thrust sheets (fault blocks) which constitute the southern section of the Valley and Ridge Province. Formations within the thrust sheet are of Paleozoic age and strike approximately 53° to the northeast and dip approximately 35° to the southeast. The thrust sheet is bounded on the northwest by the Whiteoak Mountain Fault and on the southeast by the Copper Creek Fault. Detailed descriptions of the geology are given by Stockdale (1951), McMaster (1962), and Ketelle (1982).

The site is underlain by rocks of the Cambro-Ordovician Knox Group, which includes (from oldest to the youngest) the Copper Ridge, Chepultepec, Longview, and Newala (Kingsport and Mascot) dolomites. The Knox Formations are mainly dolostones, but limestones, shales, and, occasionally, sandstone beds do occur (Harris 1971; Milici 1973).

The Knox dolostones can contain up to 50% chert, quartz grains, clay minerals, and iron-manganese oxides. Several workers (e.g., Oder and Ricketts 1961) have used the character of the chert preserved in Knox residuum to identify the parental formations from which it was derived. The sizes of chert grains range from submillimeter to boulder dimensions. Limestone-rich formations tend to weather more deeply and generally produce topographic lows.

During the Middle Ordovician Age, the Knox Group was uplifted and exposed to weathering. Solution cavities, sinkholes, subterranean drainage, and other features typical of present-day karst terranes developed during that period. More recent uplift has produced numerous joints and other fractures, and exposure of the Knox Group to surface conditions has reactivated the karst features. Numerous open passageways may be present in Knox beds, providing migration pathways for contaminants.

PEDOLOGY

Chemical weathering of the Knox Group sedimentary rocks and soil formation have been progressing for millions of years (Soil Survey Staff 1975). Four major types of parent materials occur in the soil survey area: (1) ancient alluvium of late Tertiary or early Pleistocene ages, (2) residuum from Copper Ridge, Chepultepec, Longview, and Newala members of the Knox Group, (3) old colluvium derived from the upland residual soils, and (4) younger colluvium and alluvium of late Pleistocene (Wisconsinian) and Holocene ages.

The ancient alluvium is identified by a dark red subsoil that contains an abundance of 1- to 2-mm iron-manganese nodules and concretions. The nodules and concretions formed when the alluvium was young and had a fluctuating water table. Today, erosion has resulted in landscape inversion, which has left this ancient alluvium occupying the highest elevations of the soil survey area.

Residuum soils are identified by the geologic formation in which they are presumed to have formed. Soil No. 2 is found over the Longview member. This soil is cherty throughout the profile, and chert boulders and ledges typically occur at the ground surface. Soils Nos. 5 and 5a are presumed to have formed in the Copper Ridge member. These soils have a cherty lag gravel concentrate overlying a reddish clay subsoil that contains very little chert. Soil No. 5a does not have a cherty surface.

Soil No. 4 formed in the Chepultepec member. This soil has a lag chert concentrate overlying a brown clay subsoil mottled with yellow.

Soil No. 7 formed in the Kingsport part of the Newala member. This soil has red clayey subsoil that contains considerably higher amounts of weathered soft chert than other soils.

At least two major episodes of geomorphic instability are recorded by colluvium in the soil survey area. These events are tied to early and middle Pleistocene glaciations when considerable mass movement of soil material occurred. This colluvium mantles a large part of the soil survey area. Soil No. 1 identifies colluvium in which a lithologic and/or time discontinuity at a depth of 50 cm to 2 m is a common feature. The discontinuity separates two episodes of colluviation or

of colluvium overlying residuum. The discontinuity has caused the perching of water, and a soil horizon with some properties of a fragipan has formed in response.

Soil No. 8 represents areas of younger middle and late Pleistocene alluvium. These soils occupy fan terrace landforms.

Soil No. 6 represents a variety of soils and drainages in present drainageways and heads of drains. The uppermost meter of soil is a product of post-European-settlement deposition. Many areas have a buried soil.

The soil survey indicates that a transverse fault crosses the survey area delineated by the abrupt eastern boundary of soil No. 3. (Fig. 1). In addition, the location of drainageways parallel and perpendicular to the strike of the formations also indicates the presence of transverse faults.

Classification of the soils in the survey area is given in Table 1. Brief descriptions of each soil mapping unit shown in Fig. 1 by H. C. Monger, Soil Scientist, University of Tennessee, are given below:

Soil No. 1 (Copper Ridge and Chepultepec Colluvium)

This soil is moderately well to somewhat poorly drained due to fragic properties in subsurface horizons. It formed in colluvium that collected on foot slopes, saddles, sinkholes, and on the gently sloping sides of ridges. Except for some minor areas, it has a high chert content throughout the soil profile. The fragipan, usually formed in the lithologic discontinuity, has an advanced degree of development

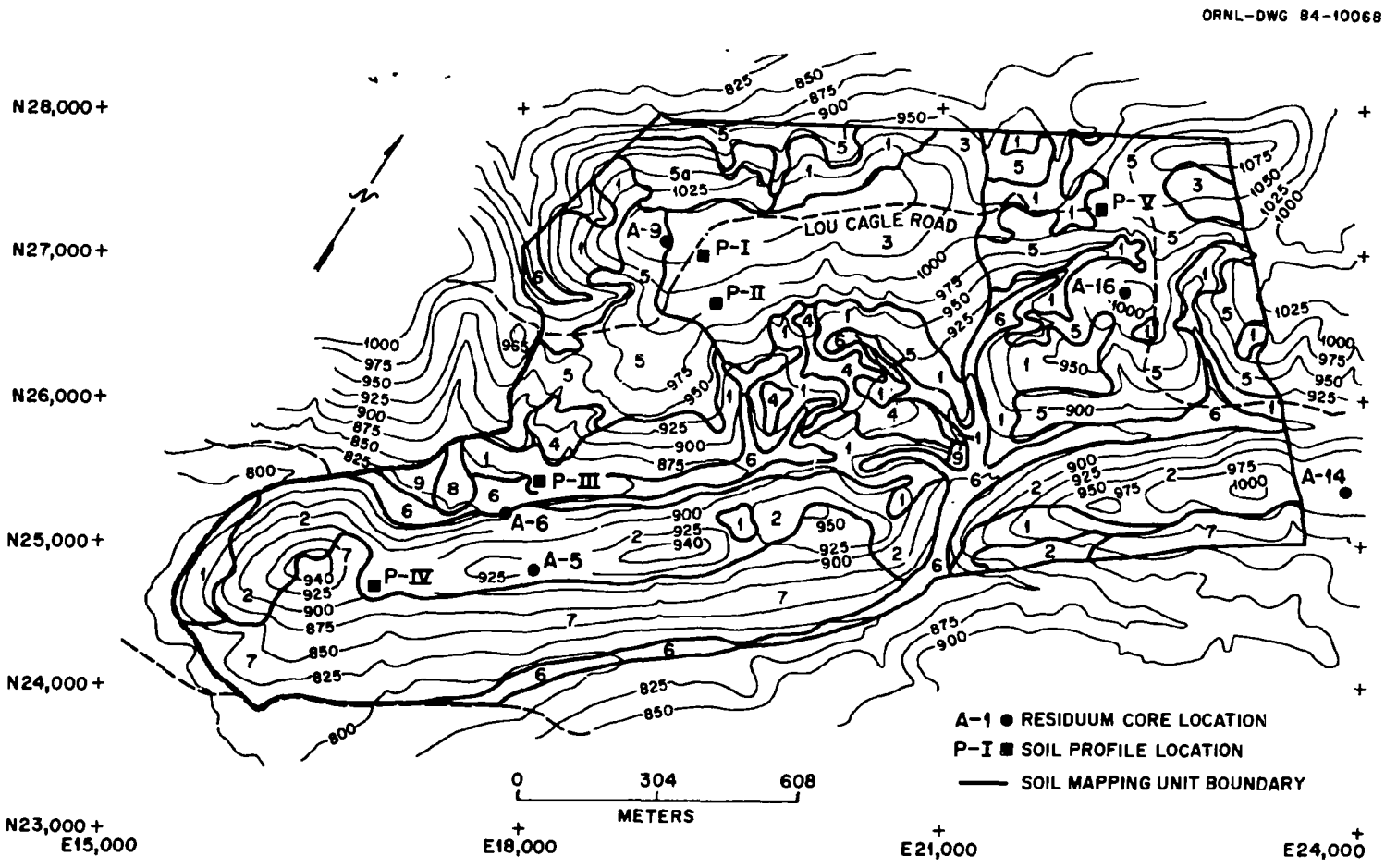

Fig. 1. Soil survey map and the locations of soil profiles and boreholes in the proposed Central Waste Disposal Facility area.

Table 1. Classification of soils in the proposed site of the Central Waste Disposal Facility

Soil No.	Classification	Series[a]
1	Fine-loamy, siliceous, thermic, Fragic Paleudult	Shack
2	Clayey-skeletal, mixed, thermic, Typic Paleudult	SND
3	Fine-loamy, oxidic, thermic, Typic and Rhodic Paleudults	Dewey and Decatur variants
4	Clayey, mixed, thermic, Paleudults	SND
5, 5a	Clayey, mixed, thermic, Paleudults	SND
6	Entisols and Inceptisols -- undifferentiated	SND
7	Fine-loamy, siliceous and clayey, kaolinitic Typic Paleudult	SND
8	Fine-loamy, siliceous, thermic, Paleudults	Holston
9	Fine-loamy, siliceous, thermic, Paleudults	Etowah

[a]SND = series not determined.

Note: Soil Nos. 2, 5, 5a, and the clayey part of No. 7 would have been included in the Fullerton Series of past mapping. They are now variants due to mixed clay mineralogy, lack of sufficient chert in the family control section, or yellow mottling in the subsoil too close to the surface. These soils were also kept separate in order to evaluate whether individual dolomite formations gave rise to similar or dissimilar soils.

ORNL/TM-9361

where this soil occurs on low toe slopes. This soil grades into soils Nos. 2 and 5 where side slopes meet ridge tops and where slopes become too steep for colluvium to collect.

Soil No. 2 (Longview Soil)

This well-drained soil is mostly underlain by the Longview Dolomite. It is very cherty throughout the entire profile, which distinguishes it from soil No. 5. It has a gray E horizon, which begins just below the leaf litter, and a red clayey subsoil beneath containing abundant chert gravels and cobbles. Chert boulders are visible on the surface in many areas.

Soil No. 3 (Ancient Alluvium)

This soil has a dark brown A horizon and a deep, dark red, silty clay loam subsoil with low chert content. It occupies the ridge top and southeastern side slope of the northwesternmost ridge in the study area. It is adjacent to soil Nos. 5 and 1, which have relatively abrupt boundaries. In some level and depressed areas, a fragipan has formed, but this is minor in extent. Pebble-size chert and iron-manganese nodules are common in the profile.

Soil No. 4 (Chepultepec Soil)

This soil is underlain by the Chepultepec Dolomite. It forms on a few island-type areas where the Chepultepec has not been covered by colluvium or alluvium. This soil is characterized by a strong brown clayey subsoil, and it has a high lag chert content, especially in the upper 0.6 m.

Soil No. 5 (Copper Ridge Soil)

This soil is underlain by the Copper Ridge Dolomite. It is characterized by an abrupt loss of chert below the top of the Bt2 horizon. It occurs on ridge tops and steep side slopes. It is well drained, with an E horizon beginning just below the leaf litter, and has a red clayey subsoil with yellow mottles common. Both massive oolitic chert and small chalky chert are common in the upper horizons.

Soil No. 5a (Copper Ridge--North Aspect)

This soil is distinguished from soil No. 5 because of its noticeably lower chert content. Like soil No. 5, it is well drained, has an E horizon extending to the surface, and has a clayey subsoil. Pebble-sized oolitic chert is present.

Soil No. 6 (Undifferentiated Modern and Holocene Alluvium)

This unit consists of undifferentiated alluvial soils, both Entisols and Inceptisols. Most Entisols are underlain by a buried soil within 1.5 m.

Soil No. 7 (Kingsport Soil and Colluvium over the Kingsport Formation)

This soil is underlain by the Newala Formation and occupies the eastern side of the most southerly ridge of the study site. It has a brown, silty A horizon and a clayey subsoil, which gradually becomes redder with depth. It has a low chert content; however, in many places Longview chert has moved downslope and covered its surface. The chert in the profile is white, pebble-size, and highly weathered. The included colluvial soils typically do not have a subsoil horizon with fragipan properties.

Soil No. 8 (Late Pleistocene Alluvium)

This soil formed in an alluvial fan which occurs near the New Zion Cemetery. It has a loamy brown A horizon with a brown clay loam subsoil.

Soil No. 9 (Late Pleistocene Terrace)

This soil formed in toe slope colluvium and alluvium. It has a dark brown A horizon and a subsoil that is reddish silty clay grading to a clay loam. Most of it lies adjacent to soil No. 8 on the southwestern side of the survey area.

MATERIALS

Samples were selected from five soil profiles in different locations within the boundary of the proposed site of the Central Waste Disposal Facility (Fig. 1). The soil profiles represent the major soil series of the site. Profile I represents Dewey variant series (Typic Paleudult, fine-loamy, oxidic, thermic); profile II represents Decatur variant series (Rhodic Paleudult, fine-loamy, oxidic, thermic); profile III represents Shack series (Fragic Paleudult, fine-loamy, siliceous, thermic); profile IV represents Fullerton variant (Typic Paleudult, clayey-skeletal, mixed, thermic); and profile V represents noncherty Fullerton variant (Typic Paleudult, clayey, mixed, thermic) (Soil Survey Staff 1975). Detailed descriptions of the soils in each profile are given in Appendix A. Three soil samples from different horizons of profiles I through IV were chosen for detailed mineralogical investigation.

Six residuum (parent material) samples were selected from five different soil cores from boreholes located within the Copper Ridge, Chepultepec, and Longview dolomite outcrop belts (Fig. 1). The residuum cores selected for analyses are from the interval close to the underlying bedrock. Detailed descriptions of the borehole cores are given in a separate report prepared by Woodward-Clyde Consultants (1984).

METHODS

Each air-dried soil and residuum sample was gently crushed with a plastic roller and passed through a 2-mm sieve. The gravel-size fraction (>2 mm) was washed with demineralized water and dried for morphological investigations. The pH of the clay fraction of soils and residuum (<2 mm) was determined in demineralized water and exchangeable cations were determined with a 1 M potassium chloride (KCl) 1:1 solid-to-solution ratio after a 2-h equilibration.

For mineralogical analyses, the <2-mm fractions were treated with 1 M sodium acetate (NaOAc) buffer solution (pH 5) to remove soluble salts and carbonates, and then with hydrogen peroxide (H_2O_2) to remove organic matter. The sand, silt, and clay fractions were separated by wet sieving, sedimentation, and centrifugation (Jackson 1975). Amorphous iron oxides in the clay fraction were removed by citrate-bicarbonate-dithionite (CBD) treatments (Mehra and Jackson 1960). Cation exchange capacities (CEC) were determined to provide an estimate of vermiculite content, assuming the vermiculite CEC was

154 meq/100 g (Alexiades and Jackson 1965). The clay fractions were fused with lithium borate ($LiBO_2$) powder and dissolved in 6 N hydrochloric acid (HCl), and then major elemental components were determined by ion-coupled argon-plasma (ICP) analysis. Mica content was calculated from total potassium oxide (K_2O) data, assuming that the mica had 10% K_2O by weight in its structure and that there were no potassium feldspars in the clay fractions.

Kaolinite content was estimated from the relative endothermic peak area (500-550°C) of the sample as compared to the peak area of poorly crystallized kaolinite standard (KGa-2, Standard Clay Mineral Repository, Clay Minerals Society), using differential scanning calorimetry (DSC). For the qualitative confirmation of the mineral distribution, the clay fractions were examined by X-ray diffractometer (XRD), using monochromatic CuKα radiation after potassium saturation and heating to 300 and 550°C, and magnesium saturation and glycol solvation.

The clay fractions were also examined by transmission electron microscopy (TEM) with an energy-dispersive X-ray detector (EDX) for morphological and qualitative elemental analyses (Lee et al. 1983b). Minerals in the silt fractions of the samples were identified by XRD. The morphology and mineralogy of sand and gravel fractions were determined by examination with an optical microscope.

RESULTS

SOIL PROPERTIES

Physical and Chemical Analysis

Soil profile I developed on old alluvium deposited over residuum of the Copper Ridge Dolomite. The soil is dark reddish brown in surface horizons and dark red in diagnostic subsurface horizons. The texture of the soil varies from clay loam to silty clay loam (Table 2). The proportion of chert fragments is low (1 to 7%) in the profile. The soil is relatively porous down to 120 cm and contains many 1- to 2-mm iron-manganese nodules.

Profile II developed on old silty alluvium over sandy residuum probably weathered from sandstone strata which start at 80 cm below the soil surface. The mixed zone of the two lithologies contains lag gravel of weathered chert. The surface horizons are dark brown, and subsurface horizons are dark red with many blackish iron-manganese nodules. The texture of the soil changes from loam to clay loam and sandy clay loam, reflecting the translocation of clays and differences in lithology within the soil profile.

Profile III was taken from a low foot slope between two drainageways; and developed on a cherty colluvium parent material. The soil varies from grayish brown to yellowish red, and fragipan is developed near a fluctuating perched water zone (2Btx/Ex horizon). The soil has a loam to clay loam texture and contains 12 to 30% coarse chert fragments. Profile IV developed on cherty dolomite residuum weathered from the Longview Dolomite formation. The soil is brown in

Table 2. Physical and chemical properties of selected samples from soil profiles

Soil map unit	Profile	Horizon	Depth (cm)	Color, Wet	pH (1:1 H_2O)	Gravel fraction, >2 mm (%)	Size distribution of <2 mm fraction (%)		
							Sand	Silt	Clay
		A	0-15	5YR3/2	6.0	3	20	52	28
Soil No. 3	I	Bt1	46-69	2.5YR3/6	4.9	7	15	53	32
		2Bt3	92-120	2.5YR4/6	4.7	5	15	49	36
		A	0-15	7.5YR3/2	5.2	6	27	47	26
Soil No. 3	II	Bt2	58-80	2.5YR3/6	4.4	3	24	41	35
		2Bt4	110-150	2.5YR3/6	4.1	1	60	17	23
		E	0-15	10YR4/2	5.3	12	34	46	20
Soil No. 1	III	Bt2	39-60	7.5YR4/4	4.3	19	34	37	29
		2Bt1	115-150	7.5YR5/6	4.6	13	42	43	15
		A	0-15	10YR4/3	5.1	27	30	51	19
Soil No. 2	IV	E	15-48	10YR5/4	4.5	45	55	27	18
		Bt2	80-150	2.5YR4/8	4.8	3	27	14	58

surface horizons and yellowish red to red in subsurface horizons. A drastic increase in clay content and decrease of in chert content were observed from the surface horizons to the subsurface horizons.

Soil pH's ranged between 5.3 and 4.1 except for the A horizon of profile I where the pH was 6.0. The higher pH is possibly the result of agricultural lime applications in the past. The pH in 1 M KCl solution was lower than the pH in H_2O because of the exchangeable acidity, aluminum plus hydrogen, in the soils.

The concentration of exchangeable aluminum varied from 1 to 20.2 mmol/kg and was relatively lower in surface horizons of the profiles (Fig. 2). A subsurface horizon of profile IV had the highest concentration of labile aluminum. The aluminum concentration increased with decreasing exchangeable calcium in the soils. The magnesium concentration showed a similar trend with decreasing exchangeable calcium, but varied less drastically within soil profiles.

Gravel and Sand Morphology

Detailed characteristics and compositions of the individual gravel and sand samples are given in Appendixes C and D, respectively. Staining is very common on the surfaces of the mineral grains in the soil samples and is evidence of weathering and oxidation. A wide range of colors from nearly white to black with many intermediate shades of orange and brown was observed. Many of the samples have an ocherous appearance.

Chert is the dominant material found in the coarser-than-sand size fraction. Several chert types were observed, including massive, oolitic, dolomoldic, porous, and banded. In many cases, the chert

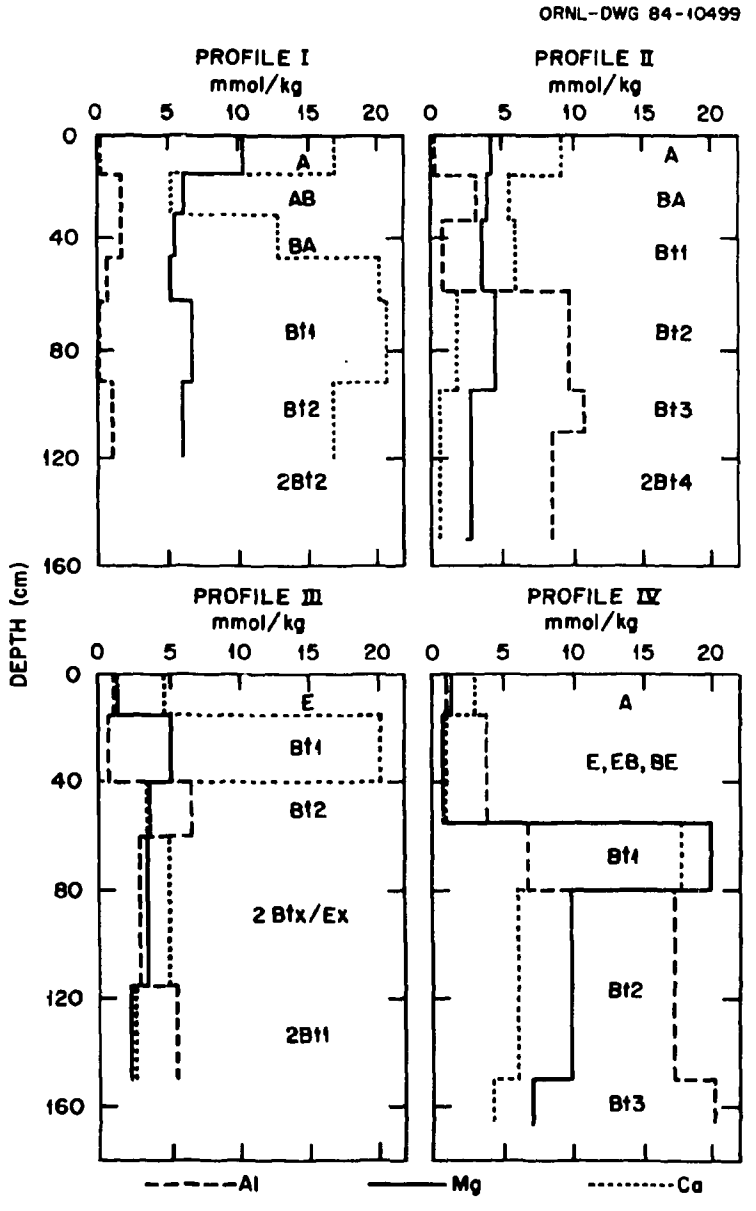

Fig. 2. Distribution of exchangeable aluminum, magnesium, and calcium in KCl(1 M) solution in the soil profiles.

showed evidence of extensive alteration to clay and/or iron-manganese nodules. In most cases, two or more types of chert were found in a single horizon. Chert grains up to 4.0 cm across were observed; however, some of these had obviously been broken, and larger fragments are likely to be encountered at the site.

Iron-manganese nodules are an important constituent of the soils in several specimens, in some cases constituting more than 50% of the specimen. Included in this category are thoroughly stained chert and rock fragments. An interesting feature of a significant number of these iron-manganese nodules is the fact that they are magnetic. These magnetic grains are shown by X-ray diffraction to contain maghemite and hematite (Fig. 3). In general, the amount of maghemite is greatest in the uppermost horizons of each pit and may be attributed to dehydration of $Fe^{2+}Fe^{3+}$ hydroxy salt (Schwertmann and Taylor 1977) which had developed in the oxidized zone of the soil horizon through the weathering of pre-existing iron-bearing minerals. Lesser amounts of maghemite were detected with a hand magnet in some of the lower soil horizons, but usually only in trace amounts. Several different types of grains that had previously been altered to iron hydroxides and then dehydrated to form maghemite were observed. Based on textural information, many of the precursor grains were various forms of chert and siltstone chips. A number of sand-size grains were noted in the coarser-than-sand size fraction. These grains were probably derived from the breakup of some of the more friable coarser grains.

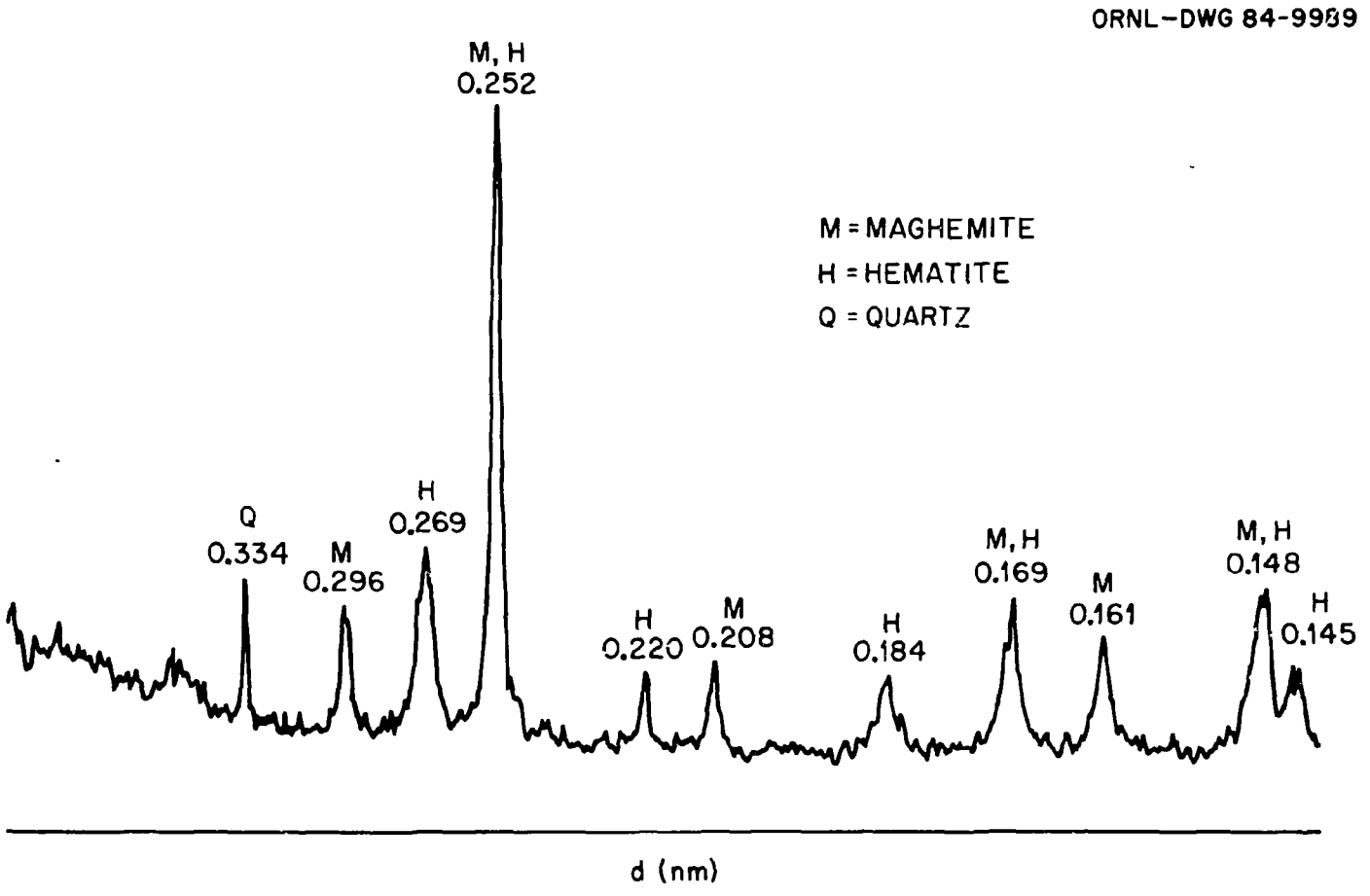

Fig. 3. X-ray diffractogram of a magnetic iron oxide nodule from the A horizon of soil profile I.

The material in the sand-size fraction ranges from very pale orange to shades of brown to almost black. The dominant mineral present is quartz in nearly clear to frosted grains. Chert grains are also common and are often stained. Several different chert types are present, including massive, porous, dolomoldic, and oolitic. Iron-manganese nodules, some magnetic, occur in amounts ranging from trace to as much as 25% of the specimen volume. Some grains show extensive alteration and appear ocherous.

Soil horizons developed in the Knox Formation are quite complex because these soils were not simply developed on top of stable Knox residuum. There is substantial evidence that material derived from the Knox Formations had been transported laterally by running water and downhill by gravity (as colluvium), washed into fractures in the rock, disrupted by farming, etc. The character of Knox soils is likely to change abruptly, both vertically and horizontally. Such differences can be observed even in the walls of a single pit.

Clay and Silt Mineralogy

The clay fractions of the soil profiles are composed of varying amounts of kaolinite, aluminum hydroxy-interlayered vermiculite (HIV), vermiculite, mica, iron oxides, gibbsite, and quartz (Table 3). Kaolinite is the most abundant mineral in the subsurface horizons, and HIV dominates in the surface horizons (A and E). Mica, vermiculite, and quartz are the next most common minerals. Amorphous iron and aluminum oxides, gibbsite, and crystalline iron oxides (hematite and maghemite) are minor (<10%) components.

Table 3. Mineralogical composition of the clay fractions (< 2μm) from selected horizons of soil profiles[a]

Profile	Horizon	Mineralogical composition (%)							
		Fe_2O_3[b]	Al_2O_3[b]	Gibbsite	Kaolinite	Mica	Vermiculite	HIV[c]	Others[d]
I	A	6.5	1.9	1.0	20	5	11	30	Qtz
	Bt1	8.3	1.1	2.0	30	5	10	25	Qtz
	2Bt3	8.4	0.8	Trace	35	6	13	15	Qtz
II	A	5.8	1.5	2.0	20	11	10	25	Qtz
	Bt2	7.2	0.7	0.2	35	12	9	20	Qtz
	2Bt4	9.2	0.9	0	40	13	9	10	Qtz, Crt
III	E	4.0	1.6	1.0	10	10	9	25	Qtz
	Bt2	5.1	0.8	1.0	20	14	10	10	Qtz
	2Bt1	4.0	0.8	0.7	20	13	13	15	Qtz
IV	A	5.0	1.7	3.5	10	10	9	40	Qtz
	E	4.5	1.3	3.0	10	12	9	40	Qtz
	Bt2	6.0	0.7	0	40	18	10	5	Qtz

[a]105°C oven-dry-weight basis.

[b]Free oxides extractable by citrate-bicarbonate-dithionite treatment.

[c]HIV = aluminum hydroxy-interlayered vermiculite estimated from X-ray diffraction intensity.

[d]Qtz = quartz and chert; crt = cristobalite.

In the clay fraction of soil profile I, the amounts of iron oxide increased and aluminum oxide decreased with increasing depth (Table 3). The HIV mineral, identified by the presence of 1.4 nm of d(001) spacing with potassium saturation at 25°C and partial collapse toward 1.0 nm after heating at 300°C and 550°C (Fig. 4), decreased with increasing depth. The major portion of the interlayered hydroxy species would be $Al(OH)_x$ polymer (Rich and Obenshain 1955; Tamura 1957; Huang and Lee 1969). In the upper part of the profile (A and Bt1 horizons), 1 to 2% gibbsite was detected by differential scanning calorimetry (DSC) spectra (not shown). There were no noticeable changes in mica and vermiculite contents within the profile. Both XRD and DSC analyses indicate the presence of relatively large quantities (20 to 35%) of kaolinite in the clay fraction. The relative intensity of 1.4- and 0.72-nm peaks of the XRD patterns of different horizons after potassium saturation clearly illustrates that the kaolinite content increases as the HIV mineral decreases with depth.

The transmission electron micrographs show the differences in mineralogical composition between samples (Fig. 5). The population of well-defined pseudohexagonal kaolinite platelets was lower in the A horizon (Fig. 5a) than in the 2Bt3 horizon (Figs. 5b and 5c) of profile I. Irregularly shaped large particles in the micrographs are micaceous minerals including HIV and vermiculite. The micrograph of the 2Bt3 horizon clay sample before citrate-bicarbonate-dithionite (CBD) treatment shows the presence of discrete fine iron oxide particles (Fig. 5c). The CBD extraction appeared to remove the discrete iron oxide particles as well as amorphous iron coatings (Jackson et al. 1973).

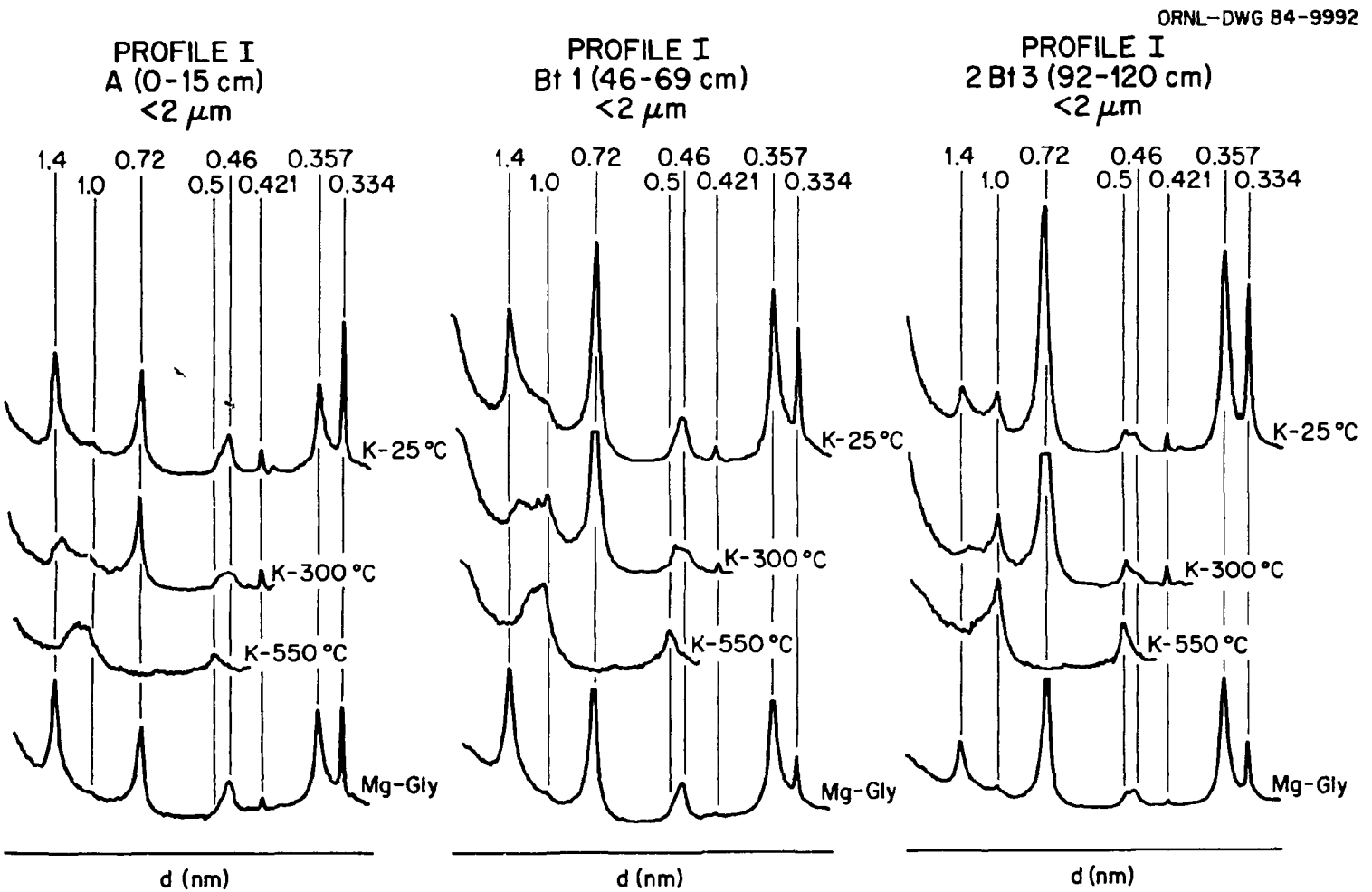

Fig. 4. X-ray diffractograms of the clay fractions (<2 μm) from selected horizons of soil profile I.

Y-197001

Fig. 5. Transmission electron micrographs of the clay fraction (<2 μm) from (a) horizon A, (b) horizon 2Bt3 after citrate-bicarbonate-dithionite (CBD) treatment, and (c) horizon 2Bt3 before CBD treatment of profile I; and from (d) horizon A, (e) horizon Bt2 without CBD treatment, and (f) horizon 2Bt4 of profile II.

The mineralogical composition of the clay fractions in soil profile II is very similar to that in profile I, the only difference observed being the higher amount of mica estimated from total elemental analyses in profile II (Table 3). The profile II clays were high in kaolinite and HIV minerals (Fig. 6). The aluminum hydroxy interlayering of vermiculite was less pronounced in the 2Bt4 horizon clay than in the surface horizon clay, suggesting that the weathering of micaceous minerals was not as advanced in the lower horizons. Kaolinite in the A horizon appeared to be degraded (Fig. 5d), whereas in the Bt2 and 2Bt4 horizons, the kaolinite particles appeared to remain as well-defined pseudohexagonal platelets (Figs. 5e and 5f). Aggregates of iron oxide minerals were observed prior to CBD treatment (Fig. 5e), and small (0.1 μm) cubic maghemite crystals were also observed in the clays after CBD treatment (Fig. 5f).

Soil profile III appears to have been leached extensively by vertically and laterally moving waters. The clay fraction of the E horizon had a well-defined HIV mineral peak (1.4 nm after potassium saturation), which collapsed only partially after subsequent heat treatments (Fig. 7). The intensities of the kaolinite peaks (0.72 and 0.357 nm) were relatively weak, and DSC analysis suggested that the kaolinite content was <10% (Table 3). The intensities of the quartz peaks at 0.42 and 0.334 nm were relatively strong, indicating a high quartz content. High quartz and low kaolinite contents resulted in a high silica-to-alumina ratio in the total chemical composition of the clay (Appendix B).

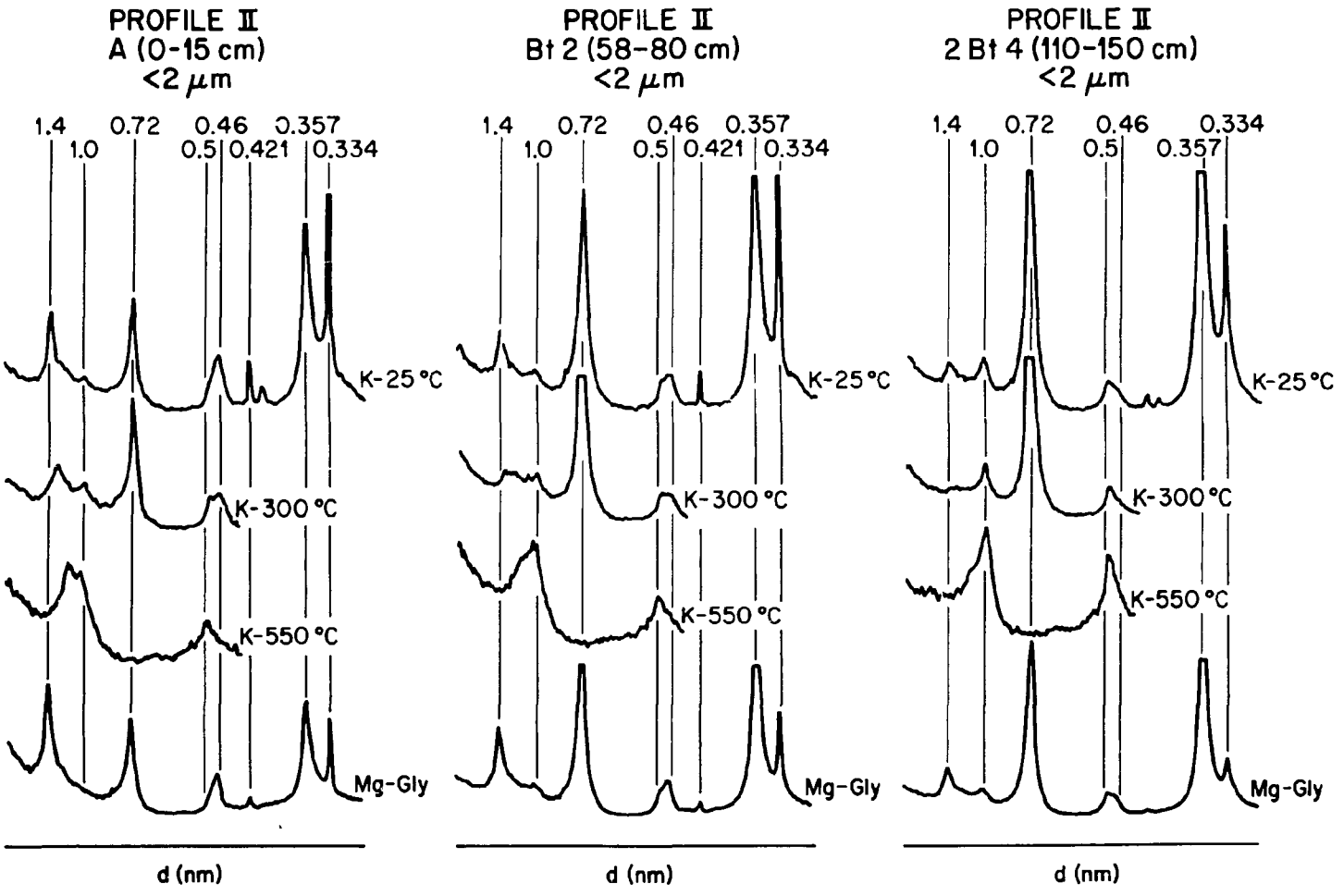

Fig. 6. X-ray diffractograms of the clay fractions (<2 μm) from selected horizons of soil profile II.

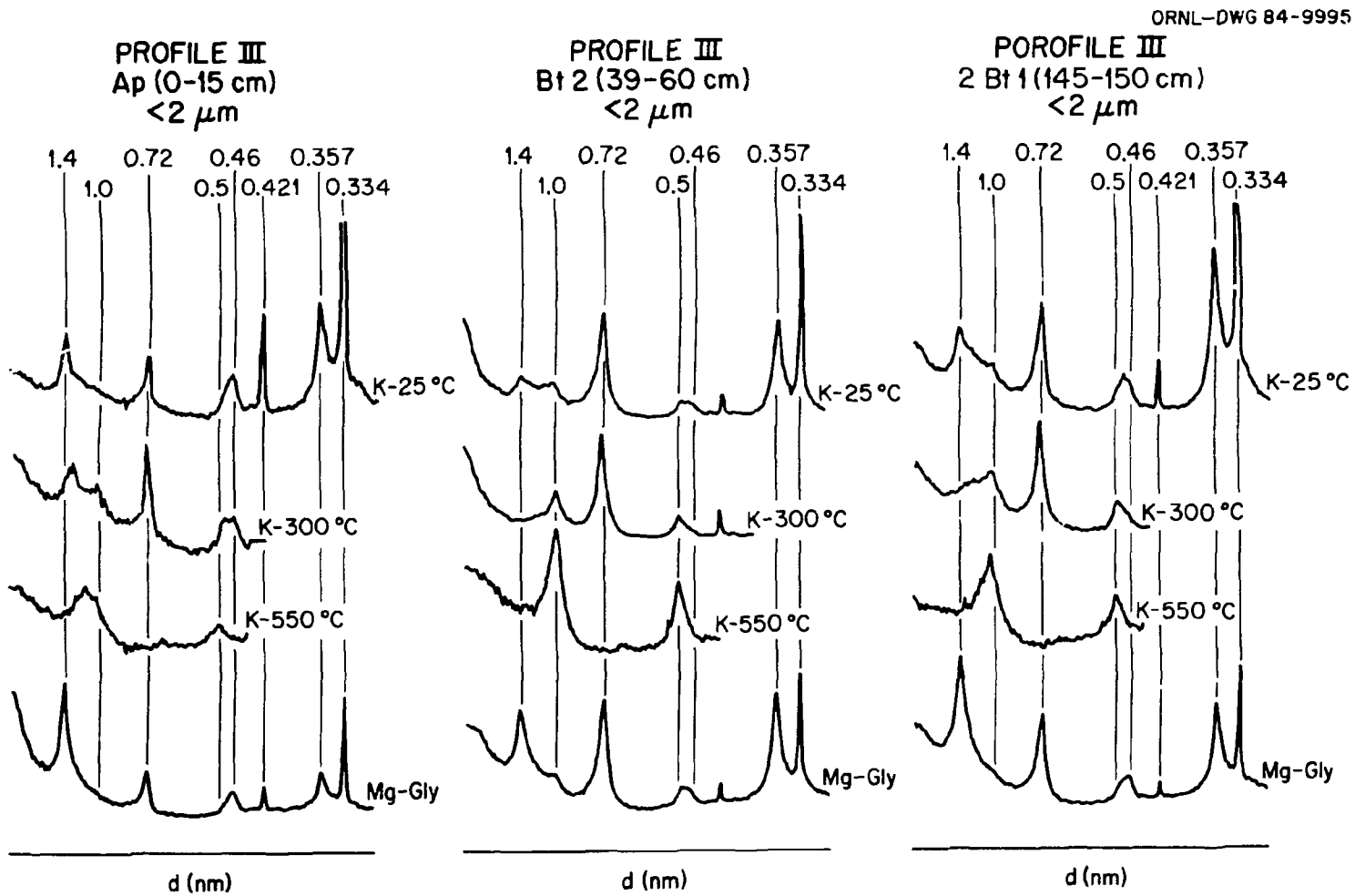

Fig. 7. X-ray diffractograms of the clay fractions (<2 μm) from selected horizons of soil profile III.

Clays in the Bt2 and 2Bt1 horizons had less well defined 1.4-nm peaks, which collapsed to 1.0 nm after heat treatments (Fig. 7), suggesting a low HIV content, and they were higher in kaolinite content than the E horizon clay (Table 3). The mica and vermiculite contents were 9 to 14% in the profile III clays. Profile III was lower in CBD-extractable amorphous sesquioxides but had about 1% crystalline gibbsite.

In soil profile IV, the clay mineral distribution changes significantly between surface and subsurface horizons (Table 3). The A and E horizons had low (10%) kaolinite content and very high (40%) stable HIV mineral content in contrast to the Bt2 horizon, which had high (40%) kaolinite and very low (10%) HIV content. The A and E horizons also had a high (3%) gibbsite content relative to the Bt2 horizon.

In the Bt2 horizon, vermiculite was partially interlayered with aluminum hydroxide and collapsed readily to 1.0 nm after potassium saturation (Fig. 8). The presence of a strong 1.0-nm XRD peak in the magnesium-glycol-solvated sample confirms the high mica content estimated from the percent of K_2O in the total chemical composition of the clay fraction in the Bt2 horizon.

The mineralogical composition of the silt fractions (50-2 μm) of the 12 soil samples from 4 soil profiles were determined by XRD. The silt fractions were composed of >80% quartz grains and <10% mica, and there were trace amounts of kaolinite and iron oxide minerals.

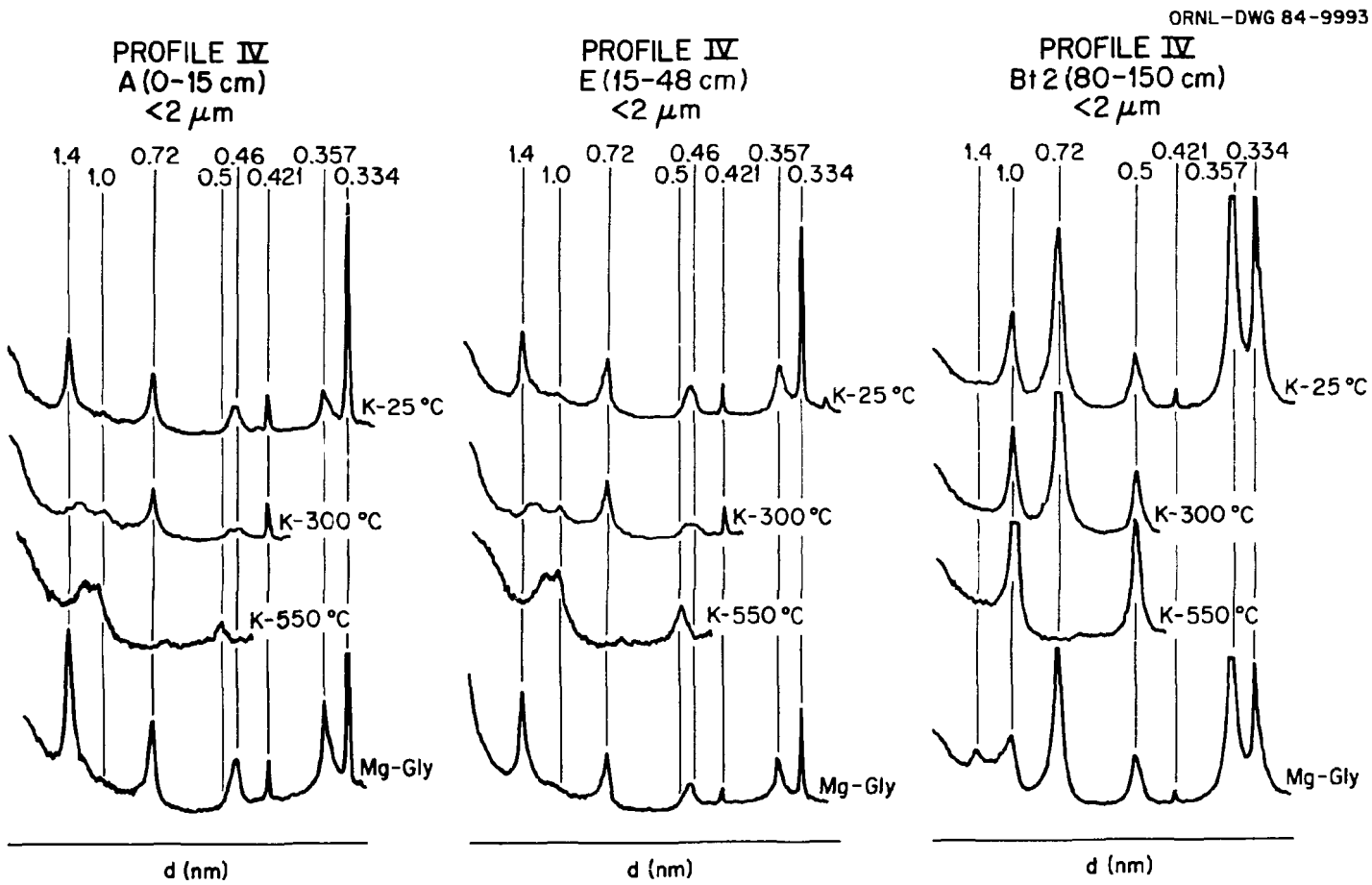

Fig. 8. X-ray diffractograms of the clay fractions (<2 μm) from selected horizons of soil profile IV.

RESIDUUM PROPERTIES

Physical and Chemical Analysis

Six samples from the five residuum borehole cores were selected for characterization. The properties and depths of the selected residuum sections are given in Table 4.

The residuum sample from borehole A-5 was red clay mixed with a small amount of yellowish weathered shale, siltstone fragments, and small amounts of gravel-size chert. The reddish clay was chosen for analysis because it was the major constituent in the section. The sample selected from core A-6 was yellowish red and had a clay loam texture with a large quantity of gravel-size chert fragments. The A-6 sample appeared to be colluvium rather than *in situ* residuum. Two sections were chosen at different depths from core A-9: the sample (denoted as A-9s) from the 23.6- to 24-m section was a weathered, very pale brown shale with a clay texture; the other sample (A-9d) from the 29.6- to 30.0-m section was a reddish-brown dolomite residuum with a clay texture.

The sample from core A-14 had many small (<1 cm), very pale brown, weathered shale fragments in a yellowish-red residuum matrix. It had a clay texture and contained <15% silt plus sand. The sample from core A-16 had a reddish matrix containing yellowish-brown, weathered siltstone fragments coated with black manganese oxides on the edges of the fragments.

The pH's of the residuum ranged between 5.0 to 6.7, slightly higher than the pH's of the soils developed from them (Tables 2 and 4). As was suggested by the pH's, A-6, A-9s, and A-9d had high

Table 4. Physical and chemical properties of selected sections from residuum cores

Core No.	Depth (m)	Color, wet	pH (1:1 H_2O)	Gravel, >2 mm (%)	Size distribution of <2-mm fraction (%)			Exchangeable concentration[a] (mmol/kg)		
					Sand	Silt	Clay	Ca	Mg	Al
A-5	13.2-13.7	2.5YR4/6	5.0	1	1	26	73	1.3	0.9	1.2
A-6	20.6-21.0	5YR5/6	6.7	42	27	40	33	3.8	3.3	0.1
A-9s	23.6-24.0	10YR7/4	6.3	14	7	33	60	2.8	2.2	0.1
A-9d	29.6-30.0	5YR4/4	6.6	1	11	5	84	3.8	3.1	0.1
A-14	11.6-12.0	5YR5/5	5.1	1	4	10	86	0.6	0.3	1.3
A-16	27.0-27.5	5YR4/4	5.4	1	5	32	63	1.4	1.2	0.4

[a]Concentration of exchangeable calcium, magnesium, and aluminum in KCL (1 M) solution.

concentrations of exchangeable calcium and magnesium but very low concentrations of exchangeable aluminum in 1 M KCl solution. The other samples had higher concentrations of exchangeable aluminum, but these concentrations were lower than those in the subsurface soils studied (Fig. 2).

Gravel and Sand Morphology

The coarser-than-sand fractions were first examined in an unwashed condition. Most were covered with ferruginous, clay like material ranging from yellowish orange to shades of brown. When washed, the underlying grains were more fully exposed, revealing a wide range of grain sizes, colors, and morphologies. The largest size noted was about 2.5 cm; however, chert grains and fragments of much greater dimensions should be anticipated at the site. The colors observed ranged from nearly pure white to various shades of yellow, orange, brown, gray, and black. The color(s) could often be related to the oxidation state of the coating material.

The dominant mineral in the coarse fraction is chert. It occurs in several types, including massive (sometimes porcelaneous), oolitic, dolomoldic, porous, etc. More than one type of chert may occur in what appears to be a single grain. The chert has been weathered or altered in different ways, including what appears to be the development of clay minerals and various iron-manganese oxides, which diffused into porous zones in the chert. In some cases, the different chert components undergo different types of alteration. For example, some oolitic

cherts that appear to be partially replaced by iron-manganese oxides also appear to be releasing fresh, unaltered grains of quartz from within the oolites.

Most of the quartz grains found in the residuum are in the sand-size range; however, a few larger grains occur, and clusters of authigenic quartz crystals occur in the gravel fractions. The authigenic clusters are thought to have formed in the Knox dolostones after they were deposited.

The numerous dark brown to almost black grains found in this fraction are iron-manganese oxide nodules. In many cases, this dark color turned out to be only a surface stain. Some of the large, dark grains disaggregated when the specimens were washed in water to remove the clay coating.

Finally, a few pieces of siltstone (or fine sandstone) were observed which are presumed to have derived from beds of these lithologies in the dolostones.

In general, similar material was observed in the sand-size fraction; however, quartz and iron-manganese nodules are present in greater amounts and in some specimens are the dominant phases. Some of the iron-manganese nodules may have originally been part of larger particles that were disaggregated during sample preparation and handling.

Many quartz grains are relatively well rounded, although a complete range of "roundness" from angular to well rounded was observed. Many of the quartz grains exhibit frosted surfaces, which some researchers interpret as being windblown material.

The chert grains present represent all chert types found in the larger size fraction. Many of the grains appear to be stained or altered, and there is a tendency for the more altered cherts to break up into finer particles.

Descriptions of the individual specimens are given in Appendixes C and D. A wide range of grain sizes, shapes, and degree of alteration and staining, etc., should be anticipated throughout the Knox residuum. The character of the material will be determined by the original mineralogy of the Knox Formations, the extent of weathering and other alteration, and the extent and nature of infusions of material through fractures and other openings in the rock.

Clay and Silt Mineralogy

In the residuum samples, kaolinite is the dominant mineral of the clay fractions, ranging from 30% to as much as 55% (Table 5). Other mineral components include mica, vermiculite, quartz, and amorphous iron and aluminum oxides. Amorphous iron and aluminum oxide coatings constituted <8% of the clays, but they effectively reduced the CEC of the clays. After removal of the oxides by citrate-bicarbonate-dithionite (CBD) treatment, the CEC of the clays increased >50% (Table 6). The clay fraction of the sample from core A-5 contained 26% vermiculite and 20% mica, and showed both 1.4- and 1.0-nm peaks in the XRD after magnesium-glycol solvation (Fig. 9). The 1.4-nm vermiculite peak collapsed to 1.0 nm after potassium saturation and heating, and the asymmetrical shape of the 1.0-nm peak indicated a partial aluminum hydroxy interlayering with the vermiculite.

Table 5. Mineralogical composition of the clay fraction (<2 μm) from selected sections of residuum cores[a]

Core No.	Mineralogical Composition (%)					
	Fe_2O_3[b]	Al_2O_3[b]	Kaolinite	Mica	Vermiculite	Others[c]
A-5	7.1	0.8	35	20	26	Qtz, HIV
A-6	5.6	0.7	35	19	20	Qtz, HIV
A-9s	2.7	0.4	30	26	8	Qtz
A-9d	5.4	0.6	55	17	6	Qtz
A-14	5.3	0.8	35	20	12	Qtz
A-16	5.6	0.6	45	14	15	Qtz

[a]105°C oven-dry-weight basis.

[b]Free oxides extractable by citrate-bicarbonate-dithionite treatment.

[c]Qtz = quartz; HIV = aluminum hydroxy-interlayered vermiculite.

Table 6. Cation exchange capacities of the c[illegible]ıctions of residua before and after citrate-bic[illegible] - dithionite (CBD) treatments

Treatment	Sample (mmol Ca/Kg)					
	A-5	A-6	A-9s	A-9d	A-14	A-16
Before CBD	85	70	40	45	75	65
After CBD	225	180	80	70	115	140

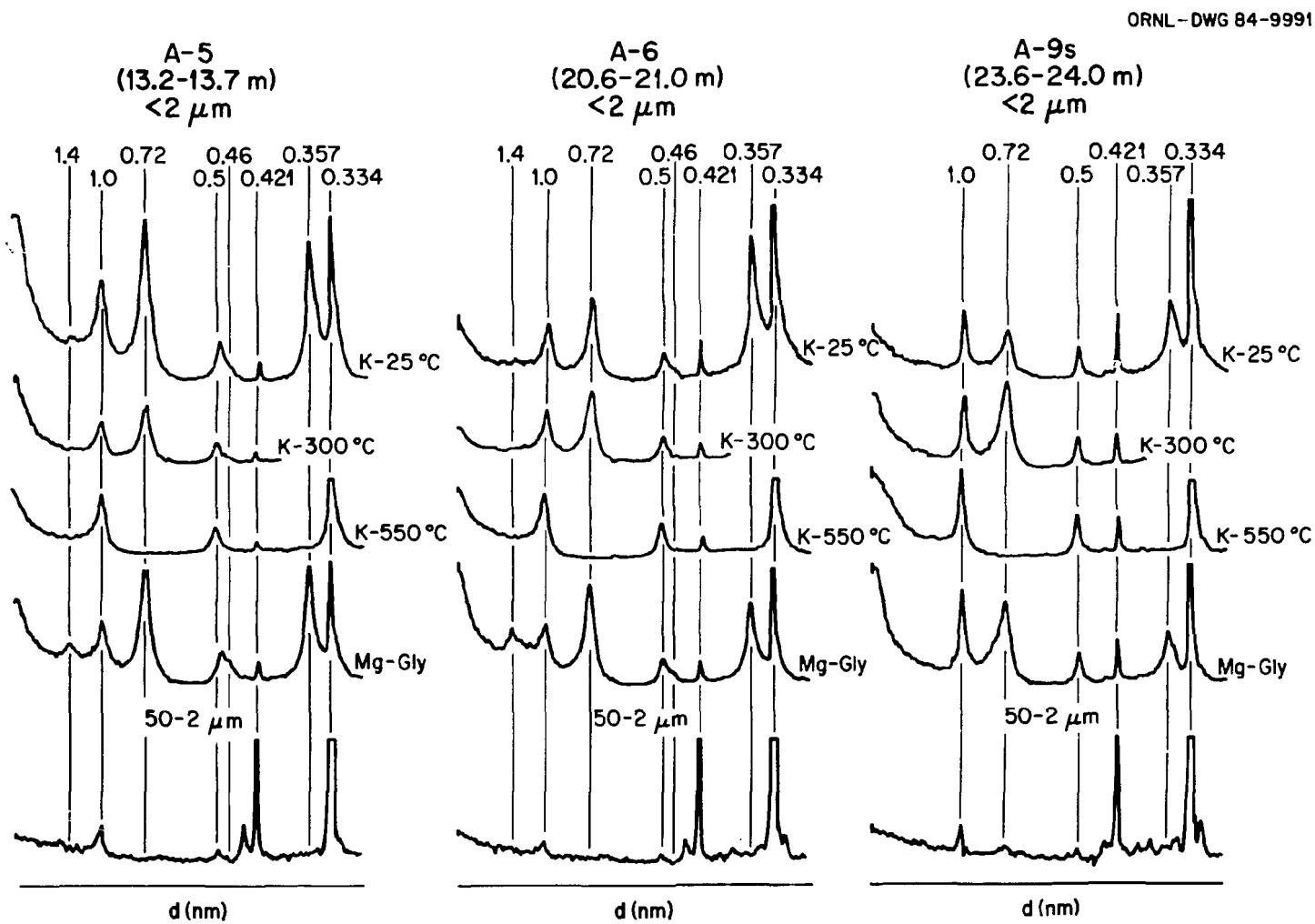

Fig. 9. X-ray diffractograms of the silt (50-2 μm) and clay fractions (<2 μm) from samples A-5, A-6, and A-9s.

The mineralogical composition of the clay fraction of the sample from core A-6 was very similar to that from core A-5. The sample from core A-6 contained 35% kaolinite, 19% mica, and 20% vermiculite (Table 5) and had similar XRD patterns (Fig. 9).

The samples from core A-9 were weathered from two different parent rocks: sample A-9s weathered from shale and contained 30% kaolinite and 26% mica; sample A-9d weathered from dolomite and contained 55% kaolinite and 17% mica in the clay fractions (Table 5). The iron and aluminum oxide contents were relatively lower in the weathered shale. Both samples had low amounts (6 to 8%) of vermiculite, resulting in an absence of 1.4-nm peaks in the XRDs (Figs. 9 and 10). The XRD patterns confirmed the results (Table 5) of semiquantitative mineralogical analyses performed independently.

The clay fraction of the sample from core A-14 was composed of 35% kaolinite, 20% mica, 12% vermiculite, and <10% quartz and amorphous iron and aluminum oxides. The XRD pattern for the sample showed a very weak 1.4-nm vermiculite peak (Fig. 10). Kaolinite dominates (45%) over other minerals in the clay fraction of the sample from core A-16; the amount of mica was 14% and vermiculite was 15%. A strong 0.72-nm kaolinite peak and weak vermiculite (1.4 nm) and mica (1.0 nm) peaks were observed in the XRD pattern of the magnesium-glycolated clay sample.

The TEM micrographs show lath-shaped illitic mica, irregular platey micas, and pseudohexagonal kaolinite in the clay fractions (Fig. 11). Kaolinite in weathered shale (sample A-9s) appeared less crystalline than that in the dolomite residuum (sample A-9d) in the

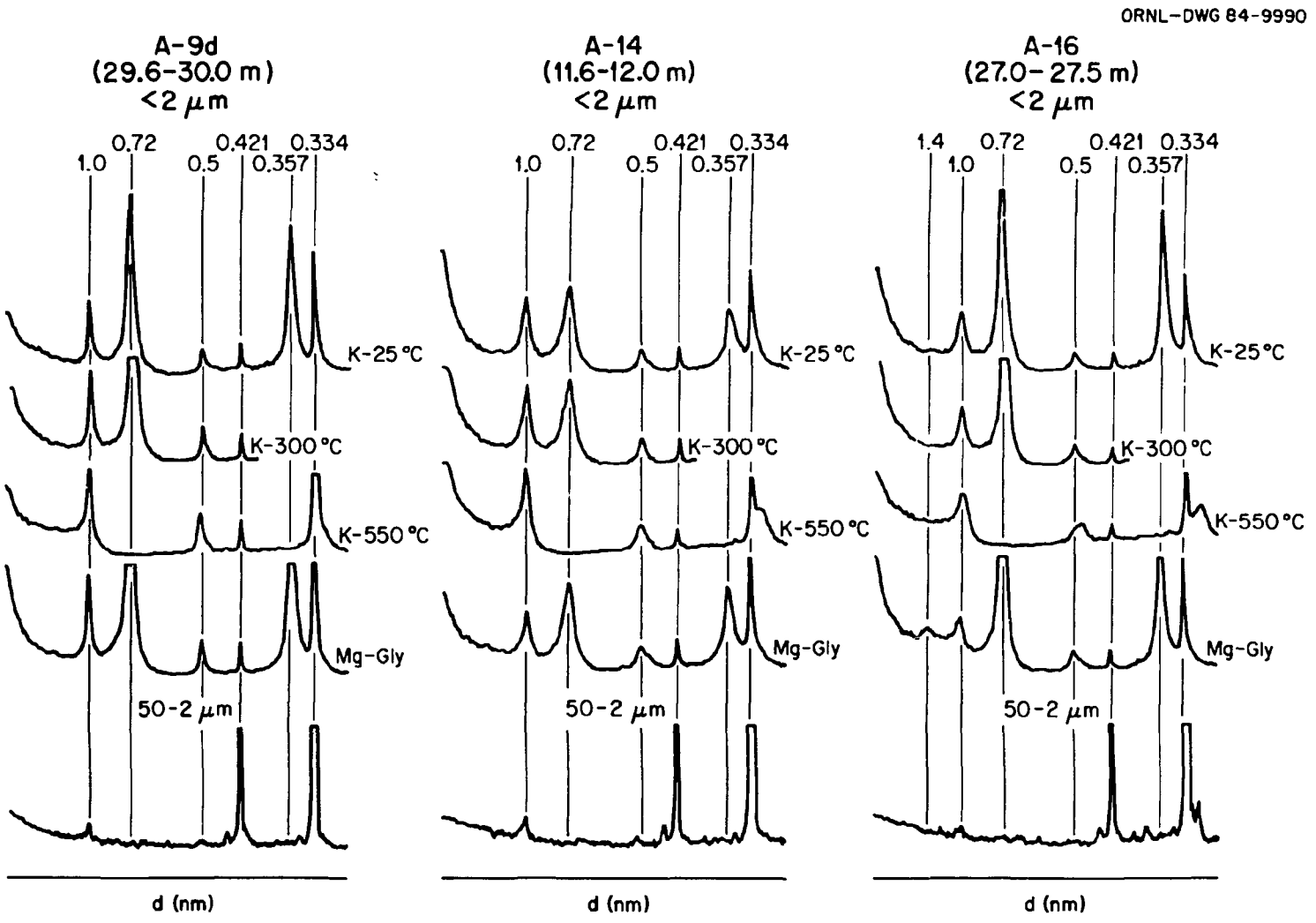

Fig. 10. X-ray diffractograms of the silt (50-2 μm) and clay fractions (<2 μm) from samples A-9d, A-14, and A-16.

Fig. 11. Transmission electron micrographs of the clay fractions (<2 μm) from samples (a) A-5, (b) A-9s, (c) A-9d, and (d) A-16.

same residuum core (Figs. 11b and 11c). The kaolinite plates dominate also in the micrograph of the clay sample from core A-16. Micrographs of other samples (not shown) were similar to the micrograph of the sample from core A-5 (Fig. 11a).

The mineralogy of the silt fraction (50-2 μm) of the residuum core samples is very simple, as is demonstrated by the XRD patterns (Figs. 9 and 10). There is >90% quartz and <10% mica in the silt fractions.

DISCUSSION

Selected soil profile and residuum samples from the proposed CWDF site were characterized by morphological, physicochemical, and mineralogical analyses. The upper horizons (<1 m) of the soil profiles may not come in contact with waste or waste leachate if shallow land burial methods are considered as a disposal technology, but the diagnostic soil horizons were included for the understanding of the pedogenesis of the soils. Information concerning ongoing pedogenesis will be a valuable reference for the assessment of the impact of any changes in geochemical environment generated by waste disposal on the physicochemical and mineralogical properties of underlying residua. The mineralogical data will provide a basis for the interpretation of geochemical (Seeley and Kelmers 1984) and hydrogeological (Ketelle and Huff 1984) investigations of the site.

The proposed site is underlain by cherty dolostone, limestone, and shale of the Cambro-Ordovician Knox Group covered by relatively thick (15-30 m) residuum (Woodward-Clyde Consultants 1984). The pedogenic

soil profiles have developed from ancient (late Tertiary) and younger (late Pleistocene) alluvium and colluvium, and from in situ residua. Soil formation, including chemical weathering of parent material and subsequent leaching of mobile components, has been progressing for millions of years. Without a drastic change in chemical environment, the pedogenesis might be expected to progress at the present rate indefinitely.

The soils studied have cherty lag gravel concentrates overlying heavy-textured subsoils. Chert is the dominant material found in the gravels, and iron-manganese coatings are very common on the surface of the grains. There were several chert types, including massive, oolitic, dolomoldic, and porous, with varying degrees of alteration. In many cases, the chert showed evidence of extensive alteration to iron-manganese oxide. The iron-manganese oxide nodules, some of which were ferromagnetic, were also significant components. The magnetic grains were a mixture of maghemite, hematite, and quartz.

In the sand fraction of the soils, the dominant minerals were quartz in nearly clear to frosted grains, chert with varying degrees of alteration, and iron-manganese oxides both with and without ferromagnetic properties. Quartz was the dominant mineral in the silt-size fraction, which also contained very small amounts (<5%) of micaceous minerals.

The different types of chert coated with varying amounts of iron-manganese oxides were major components of the gravel fractions in the residuum samples. In the sand-size fraction, the major components were quartz and chert, and quartz was the dominant mineral in the silt-size fraction.

The morphological features of the coarse grains in the soils and residua were very similar. They were a mixture of chert of different types and colors with varying degrees of stain and alteration. The most significant difference was the amount of iron-manganese oxide minerals present. The oxides tended to be in nodules in the soil samples, whereas, in the residua, most of the iron-manganese oxides were present as coatings on chert grains. The formation of iron-manganese oxide nodules through leaching and reprecipitation is commonly observed in soils in this area (Moneymaker 1981). However, the presence of magnetic iron oxide (maghemite) in the soils has not been reported.

Maghemite is not a common mineral in soils. Maghemite formation in soils has been attributed to aerial oxidation of detrital magnetite (Bonifas 1959). The chemical environments governing maghemite formation in soils are poorly understood. Somewhat reducing conditions are necessary to form an $Fe^{2+}Fe^{3+}$ hydroxy compound that might be a precursor from which maghemite is formed by slow oxidation and simultaneous dehydration (Taylor and Schwertmann 1974). Further study of maghemite is required for the understanding of the geochemical environments, especially redox conditions, needed for its formation.

The clay-size fraction is the most important constituent in the soils and residua because many physicochemical, hydrological, and mechanical properties are governed by the mineralogical composition of the clays. The proportion of clay fraction in the soils ranged from 15 to 58% and that in the residua ranged from 60 to 86%, except for the sample from core A-6, which is believed to be colluvium. The

heavy-textured materials are expected to have very low permeability, which could be desirable for limiting the mobility of leached radionuclides from the buried waste.

The clay fractions were composed of varying amounts of kaolinite, mica, vermiculite, aluminum hydroxy-interlayered vermiculite (HIV), amorphous iron and aluminum oxides, gibbsite, and quartz. In the soils, kaolinite contents increased and HIV contents decreased with depth. Micas weathered to vermiculites, and the cation exchange sites of the vermiculites were occupied by nonexchangeable aluminum hydroxides in the surface soils. The major source of interlayered aluminum was kaolinite weathering. The presence of crystalline gibbsite also indicates that the soil solutions have been oversaturated relative to gibbsite (Karathanasis et al. 1983). Some of the aluminum was adsorbed by vermiculites in the surface soils. The increase in HIV content means lower exchange capacity of the soil. However, the increase of iron and aluminum hydroxides would provide an additional sorption site for radionuclides such as cobalt and uranium. The sorption mechanism of the hydroxides is complex and differs from the ion exchange mechanism of micaceous minerals, which are dominated by permanent negative charges.

The residuum samples are relatively free of aluminum hydroxide in the interlayers of vermiculite. The residua have large amounts of mica and kaolinite, and the minerals were less altered compared to the clays in the surface soils. The fixation of radioactive cesium is expected to be more favorable in the residua because of the higher micaceous mineral content. The amounts of amorphous iron and aluminum hydroxides

in the residua are lower than the amounts found in the soils but enough to have high sorption ratios for hydrolizable radionuclides. Seeley and Kelmers (1984) report that residuum taken from the CWDF site had the highest sorption ratios they have measured for uranium in any geologic material.

The mineralogical compositions suggest that the residua are in a somewhat less advanced state of weathering compared to the surficial soils at the site. The residua have been leached (not excessively) and have low base saturation but are not oversaturated with respect to aluminum hydroxide (gibbsite). However, the fragile balance of chemical and mineralogical equilibria could be easily broken if extreme chemical conditions are introduced into the residuum. Therefore, the existing favorable physicochemical and mineralogical conditions for radionuclide retardation in the residuum can be maintained only through proper waste disposal practices.

REFERENCES

Alexiades, C. A., and M. L. Jackson. 1965. Quantitative determination of vermiculite in soils. Soil Sci. Soc. Am. J. 29:522-527.

Bonifas, M. 1959. Contribution a l'etude geochimique de l'alteration laterique. p. 159. Mem. Serv. Carte Gaol. Alsace Lorraine 17, France.

Carroll, D. 1961. Soils and rocks of the Oak Ridge Area, Tennessee. USGS Trace Elements Inv. Report, TEI-785. U.S. Geological Survey, Reston, Virginia.

Harris, L. D. 1971. A lower Paleozoic paleoquifer-- the Kingsport Formation and Mascot Dolomite of Tennessee and southwest Virgina. Economic Geol. 66:735-743.

Huang, P. M., and S. Y. Lee. 1969. Effect of drainage on weathering transformations of mineral colloids of some Canadian prairie soils. pp 541-551. Proc. Int. Clay Conf., Tokyo, Japan. Israel Universities Press, Jerusalem, Israel.

Jackson, M. L. 1975. Soil Chemical Analysis--Advanced Course, 2nd ed. Published by the author, Department of Soil Science, University of Wisconsin, Madison, Wisconsin.

Jackson, M. L., S. Y. Lee, J. L. Brown, I. B. Sachas, and J. K. Syers. 1973. Scanning electron microscopy of hydrous metal oxide crusts intercalated in naturally weathered micaceous vermiculite. Soil Sci. Soc. Am. J. 37:127-131.

Karathanasis, A. D., F. Adams, and B. F. Hajek. 1983. Stability relationships in kaolinite, gibbsite, and Al-hydroxy-interlayered vermiculite soil. Soil Sci. Soc. Am. J. 47:1247-1251.

Ketelle, R. H. 1982. Report on preliminary site characterization of the West Chestnut Ridge site. ORNL/NFW-82/21. Oak Ridge National Laboratory, Oak Ridge, Tennessee.

Ketelle, R. H., and D. D. Huff. 1984. Site characterization of the West Chestnut Ridge site. ORNL/TM-9229. Oak Ridge National Laboratory, Oak Ridge, Tennessee.

Lee, D. W., R. H. Ketelle, and L. H. Stinton. 1983a. Use of DOE site selection criteria for screening low-level waste disposal sites on the Oak Ridge Reservation. ORNL/TM-8717. Oak Ridge National Laboratory, Oak Ridge, Tennessee.

Lee, S. Y., J. B. Dixon, and M. M. Aba-Husayn. 1983b. Mineralogy of Saudi Arabian soils: Eastern region. Soil Sci. Soc. Am. J. 47:321-326.

McMaster, W. M. 1962. Geologic map of the Oak Ridge Area, Tennessee: Scale 1:31,680. U.S. Geological Survey, Reston, Virginia

Mehra, O. P., and M. L. Jackson. 1960. Iron oxide removal from soils and clays by a dithionite-citrate system buffered with sodium bicarbonate. Clays Clay Miner. 7:317-327.

Milici, R. C. 1973. The stratigraphy of Knox County, Tennessee. pp. 9-24 IN Geology of Knox County. Bulletin 70. Tennessee Division of Geology, Nashville, Tennessee.

Moneymaker, R. H. 1981. Soil survey of Anderson County, Tennessee. Soil Conservation Service, U.S. Department of Agriculture.

Oder, C.R.L., and J. E. Ricketts. 1961. Geology of the Mascot-Jefferson City zinc district, Tennessee. Report of Investigation No. 12. Tennessee Division of Geology, Nashville, Tennessee.

Rich, C. I., and S. S. Obenshain. 1955. Chemical and clay mineral properties of a Red-Yellow Podzolic soil derived from muscovite schist. Soil Sci. Soc. Am. J. 19:334-339.

Seeley, F. G., and A. D. Kelmers. 1984. Geochemical information for the West Chestnut Ridge Central Waste Disposal Facility for low-level radioactive waste. ORNL-6061. Oak Ridge National Laboratory, Oak Ridge, Tennessee.

Soil Survey Staff. 1975. Soil taxonomy: A basic system of soil classification for making and interpreting soil surveys. Agric. Handbook No. 436. U.S. Department of Agriculture, U.S. Government Printing Office, Washington, D.C.

Stockdale, P. B. 1951. Geologic conditions at the Oak Ridge National Laboratory (X-10) area relevant to the disposal of radioactive waste. p. 87. ORO-58. U.S. Atomic Energy Commission, Oak Ridge, Tennessee.

Schwertmann, U., and R. M. Taylor. 1977. Iron oxides. p. 165 IN J. B. Dixon and S. B. Weed (eds.), Minerals in Soil Environment. Soil Science Society of America, Madison, Wisconsin.

Tamura, T. 1957. Identification of the 14A clay mineral component. Am. Mineral. 42:107-110.

Taylor, R. M., and U. Schwertmann. 1974. Maghemite in soils and its origin. Parts I and II. Clay Miner. 10:289-298 and 299-310.

Woodward-Clyde Consultants. 1984. Subsurface characterization and geohydrologic site evaluaiton, West Chestnut Ridge site. ORNL/Sub/83-647641/IvI2. Prepared by Woodward-Clyde Consultants, Wayne, New Jersey, for Oak Ridge National Laboratory, Oak Ridge, Tennessee.

APPENDIX A

DESCRIPTION OF SOIL PROFILES OF PITS

APPENDIX A

DESCRIPTION OF SOIL PROFILES OF PITS

Pit No. 1

Area:	Roane County, Tennessee
Location:	West Chestnut Ridge, ORNL
Vegetation:	Red oak, white oak, hickory
Parent materials:	Old alluvium over residuum
Landform:	Upper side slope
Elevation:	322m (1060 ft)
Slope:	2-6%
Aspect:	Southeast
Erosion:	Nil
Permeability:	Moderate
Classification:	Typic Paleudult; fine-loamy, oxidic, thermic
Soil series:	Dewey variant (soil No. 3 in soil survey)
Described by:	D. A. Lietzke, University of Tennessee (12/5/83)

Soil Profile, Pit No. 1

Horizon	Depth(cm)	Description
Oi	4-2	Leaf litter
Oe	2-0	Fragment layer
A	0-15	Dark reddish-brown (5YR3/2) silt loam; moderate fine granular structure; very friable; many fine roots; 2 to 5% chert and Fe-Mn nodules; clear wavy boundary
AB	15-30	Highly mixed yellowish-red (5YR4/6) and dark reddish-brown (5YR3/4) silt loam; dark reddish-brown (5YR3/3) crushed and mixed; moderate fine granular structure, very friable; very porous; common fine roots; 1 to 3% chert fragments; common 1- to 2-mm Fe-Mn nodules
BA	30-46	Dark red (2.5YR3/6) heavy silt loam; moderate fine subangular blocky structure; very friable; common fine and medium roots; 1 to 3% chert fragments; common to many 1- to 2-mm Fe-Mn nodules; gradual wavy boundary
Bt1	46-62	Dark red (2.5YR3/6) silty clay loam; moderate medium subangular blocky structure; friable; very thin dark red (10R3/6) ped coatings; few medium roots; 1 to 10% chert fragments; common to many 1- 2-mm Fe-Mn nodules; diffuse wavy boundary

APPENDIX A (continued)

Soil Profile, Pit No. 1 (continued)

Horizon	Depth(cm)	Description
Bt2	62-92	Dark red (2.5YR3/6) silty clay loam; moderate medium subangular block structure; friable; thin slightly darker red (2.5YR3/6) ped coatings; few medium roots; 1 to 3% chert fragments; many 1- to 2-mm Fe-Mn nodules; diffuse wavy boundary
2Bt3	92-120	Red (2.5Y4/6) silty clay loam; weak coarse prismatic parting to moderate medium subangular blocky structure; friable; thin dark red (2.5YR3/6) ped coatings; common reddish-brown (5YR5/4) flow zones; and around old root channels; few medium and fine roots; 5 to 10% chert fragments; no Fe-Mn nodules; gradual wavy boundary
2Bt4	120-150	Red (2.5YR4/6) clay; weak coarse prismatic parting to moderate medium subangular block structures; friable; thin dark red (2.5YR3/6) ped coatings; reddish-brown (5YR5/4) thin flow zones around root channels; yellowish-red (5YR5/6) larger flow zones; no roots; 5 to 10% chert fragments

Note: Soil is very porous to 120 cm.

APPENDIX A (continued)

Pit No. 2

Area:	Roane County, Tennessee
Location:	West Chestnut Ridge, ORNL
Vegetation:	Hardwoods: oak, hickory
Parent materials:	Old silty alluvium over higher-sand-content residuum
Landform:	Upper side slope
Elevation:	298 m (980 ft)
Slope:	6-12%
Aspect:	Southeast
Erosion:	Nil
Permeability:	Moderate throughout
Classification:	Rhodic Paleudult; fine-loamy, oxidic, thermic
Soil series;	Decatur variant (soil No. 3 on soil survey)
Described by:	D. A. Lietzke, University of Tennessee (12/5/83)

Soil Profile, Pit No. 2

Horizon	Depth(cm)	Description
Oi	3-1	Fresh leaf litter
Oe	1-0	Fragment layer
A	0-5	Dark brown (7.5YR3/2) loam; moderate fine granular structure; very friable; many fine roots and pores; 1 to 10% fragments; clear wavy boundary
AB	15-32	Dark reddish-brown (5YR3/6) and B part dark red (2.5YR3/6) silt loam--highly mixed by soil fauna; moderate fine granular structure; very friable; common medium roots; many 1 to 2-mm pores; 1- to 5% oolitic chert gravel fragments; gradual wavy boundary
Bt1	32-58	Dark red (2.5YR3/6) silty clay loam; moderate medium subangular block structure; friable; many 1-mm spherical Fe-Mn nodules; few medium roots; common pores; 1 to 2% highly weathered oolitic chert gravels; diffuse wavy boundary

APPENDIX A (continued)

Soil Profile, Pit No. 2 (continued)

Horizon	Depth(cm)	Description
Bt2	58-80	Dark red (2.5YR3/6) clay loam; moderate medium subangular blocky structure; firm; many 1-to 2-mm, black Fe-Mn nodules; thin dark red (10R3/6) ped coatings; few red (2.5YR4/6) flow zones; few fine roots; many fine pores; 1 to 10% highly weathered oolitic chert gravels impregnated with Fe-Mn nodules; diffuse wavy boundary
2Bt3	80-110	Dark red (10YR3/6) sandy clay loam; moderate fine subangular blocky structure; friable; thin dusky red (10R3/4) ped coatings; few to common red (2.5YR4/6) flow zones; few fine roots; many fine pores; 1 to 2% chert gravel fragments; diffuse wavy boundary
2Bt4	110-150	Dark red (2.5YR3/6) sandy clay loam; weak coarse prismatic parting to weak coarse subangular blocky structure; friable; dark red (20R3/6) ped coatings; few to common strong brown (7.5YR5/6) flow zones; no roots or coarse fragments

Notes:
1. The Bt2 comprises a mixed zone of the two lithologies; it also contains lag chert gravel.
2. Most of the chert is highly weathered and is partially impregnated with Fe-Mn materials.
3. There are no Mn nodules below the discontinuity.
4. The chert lag zone extends all the way around the pit. The southeast corner of the pit contains a large concentration of gravel-sized chert, giving a clayey-skeletal particle-size class.

APPENDIX A (continued)

Pit No. 3

Area:	Roane County, Tennessee
Location:	West Chestnut Ridge, ORNL
Vegetation:	Old field succession: pine, red cedar, beech, oak
Parent materials:	Cherty colluvium over older cherty colluvium
Landform:	Low foot slope, concave perpendicular to contour, convex parallel to contour; site situated between two drainageways
Elevation:	255 m (840 ft)
Slope:	2-6%
Aspect:	South-southeast
Erosion:	Slight
Permeability:	Moderate--2Btx/Ex is moderately slow; 2Bt1 beneath is moderate
Classification:	Fragic Paleudult; fine-loamy, siliceous, thermic
Soil Series:	Shack (soil No. 1 on soil survey)
Described by:	D. A. Lietzke, University of Tennessee (12/5/83)

Soil Profile, Pit No. 3

Horizon	Depth(cm)	Description
Oi	4-2	Fresh leaf litter
Oe	2-0	Fragment layer
E	0-15	Dark grayish-brown (10YR4/2) gravelly loam; moderate fine granular structure; very friable; many fine and medium roots; 10 to 30% chert fragments; clear wavy boundary
Bt1	15-39	Yellowish-brown (10YR5/4) gravelly clay loam; moderate to fine subangular block structure; friable; thin dark yellowish-brown (10YR4/4) ped coatings; few medium roots; 25 to 50% chert fragments; gradual wavy boundary
Bt2	39-60	Brown (7.5YR4/4) gravelly clay loam; moderate medium subangular block structure; friable; yellowish-red (5YR4/6) ped coatings; some ped faces have thin black Mn coatings; few medium roots; 20 to 35% chert fragments; gradual wavy boundary

APPENDIX A (continued)

Soil Profile, Pit No. 3 (continued)

Horizon	Depth(cm)	Description
2Btx/Ex	60-115	B part yellowish-red (5YR4/6) and E part light yellowish-brown (10YR6/4) gravelly clay loam; weak coarse prismatic structure; 30 to 40% brittle zones associated mostly with Ex; remainder is friable; reddish-brown (5YR4/4) clay coats both Btx and Ex material and also occurs as thick plugs in pores; many 1- to 3-mm vesicular pores in brittle parts; few roots on prism faces and in friable material; 25 to 30% chert fragments; gradual irregular boundary
2Bt1	115-150	Strong brown (7.5YR5/6) gravelly loam; weak coarse subangular blocky structure; friable; thin red (2.5YR4/6) ped coatings; many light yellowish-brown (10YR6/4) flow zones descending from the horizon above; no roots; 10 to 20% chert fragments

Note: The fluctuating perched water rises to 90-cm level or less during rainy periods when soil water is moving laterally.

APPENDIX A (continued)

Pit No. 4

Area:	Roane County, Tennessee
Location:	West Chestnut Ridge, ORNL
Vegetation:	Tulip poplar and white oak--old field
Parent Materials	Cherty dolomite residuum of Longview Formation
Landform:	Convex portion of upper saddle
Elevation:	280m (920 ft)
Slope:	2-6%
Aspect:	East
Erosion:	Nil
Permeability:	Moderate to 100 cm, moderately slow below
Classification:	Typic Paleudult; clayey skeletal, mixed thermic
Soil series:	Fullerton variant (soil No. 2 on soil survey)
Described by:	D. A. Lietzke, University of Tennessee (12/5/83)

Soil Profile, Pit No. 4

Horizon	Depth(cm)	Description
Oi	4-2	Fresh leaf litter
Oe	2-0	Fragment layer
A	0-15	Brown (10YR4/3) very gravelly silt loam; weak fine granular structure; friable; 25 to 50% chert fragments; common fine and medium roots; clear wavy boundary
E	15-30	Yellowish-brown (10YR5/4) gravelly sandy loam; weak fine subangular blocky structure, friable; 35 to 50% chert fragments; few medium roots; gradual wavy boundary
EB	30-40	Strong brown (7.5YR5/6) gravelly clay loam; weak fine granular structure; friable; 35 to 50% chert fragments; few medium roots; clear wavy boundary
BE	40-55	Yellowish-red (5YR5/6) very gravelly heavy clay loam; weak medium subangular blocky structure; friable; 30 to 50% chert fragments; few medium roots; gradual wavy boundary

APPENDIX A (continued)

Soil Profile, Pit No. 4 (continued)

Horizon	Depth(cm)	Description
Bt1	55-80	Red (2.5YR4/8) gravelly clay; moderate medium subangular block structure; friable; thin red (2.5YR4/6) and dark red (2.5YR3/6) ped coatings; 35 to 50% chert fragments; few fine roots; diffuse wavy boundary
Bt2	80-150	Mottled red (2.5YR4/8) and yellowish-red (5YR5/6) gravelly clay; weak very coarse prismatic parting to moderate medium subangular blocky structure; firm; thin red (2.5YR4/6) ped coatings; common yellowish brown (10YR5/6) flow zones; 25 to 45% chert fragments; few fine roots; diffuse wavy boundary
Bt3	150-175	Same colors as above with moderate structure, but strike and dip of geologic strata can be discerned

APPENDIX A (continued)

Pit No. 5

Area:	Roane County, Tennesee
Location:	West Chestnut Ridge, ORNL
Vegetation:	Oak, hickory
Parent materials:	Residuum from low-chert-content Copper Ridge
Landform:	Narrow upland summit near a saddle
Elevation:	310 m (1020 ft)
Slope:	2-6%
Aspect:	South
Erosion:	Nil
Permeability:	Moderate to 95 cm; moderately slow below
Classification:	Typic Paleudult; clayey, mixed, thermic
Soil series:	Noncherty Fullerton variant (soil No. 5 on soil survey)
Described by:	D. A. Lietzke, University of Tennessee (12/5/83)

Soil Profile, Pit No. 5

Horizon	Depth(cm)	Description
Oi	4-2	Fresh leaf litter
Oe	2-0	Fragment layer
E1	0-15	Brown (10YR5/3) gravelly silt loam; weak fine granular structure; very friable; many fine roots; 15 to 50% chert fragments; gradual wavy boundary
E/Bt	15-38	E part pale brown (10YR6/3) gravelly silt loam and Bt part light yellowish-brown (10YR6/3) gravelly silty clay loam; weak fine subangular blocky structure; friable; few medium roots; 10 to 35% chert fragments; clear irregular boundary
Bt/E	38-55	Bt part strong brown (7.5YR5/6) and E part yellowish-brown (10YR5/4) gravelly silty clay loam; weak medium subangular blocky structure; friable; few fine roots; 10 to 25% chert fragments; clear irregular boundary
Bt1	55-95	Red (2.5YR4/8) silty clay; weak coarse subangular blocky structure; firm; peds coated with thin red (2.5YR4/6) material; few fine roots; 0 to 5% chert fragments; diffuse wavy boundary

APPENDIX A (continued)

Soil Profile, Pit No. 5 (continued)

Horizon	Depth(cm)	Description
Bt2	95-150	Variegated red (2.5YR4/6-4/8), yellowish-red (5TY5/6) and strong brown (7.5YR5/6) silty clay; weak very coarse prismatic parting to weak coarse subangular block structure; firm; thick red (2.5YR4/6) coats on primary ped faces; yellowish-brown (10YR5/6) flow zones; few fine roots; 2 to 10% oriented chert fragments

Notes: 1. Chert fragments are mostly massive and dark in color.

2. The 38- to 55-cm section is a degraded upper argillic horizon.

APPENDIX B

TOTAL CHEMICAL COMPOSITION OF CLAY FRACTIONS (<2 μm) FROM SELECTED SOILS AND RESIDUA

APPENDIX B

Total chemical composition of clay fractions (<2 μm) from selected soils and residua

Profile or Core No.	Horizon or depth (m)	Chemical composition of clay fractions (%)						
		SiO_2	Al_2O_3	Fe_2O_3	MgO	K_2O	TiO_2	SiO_2/Al_2O_3[a]
	A	54.1	24.4	1.7	0.9	0.5	1.3	3.8
I	Bt1	46.9	23.8	1.4	0.9	0.5	1.0	3.3
	2Bt3	59.9	27.2	1.2	0.9	0.6	1.1	3.7
	A	55.0	22.0	1.5	0.9	1.1	1.1	4.2
II	Bt2	56.3	22.7	1.0	1.1	1.2	1.0	4.2
	2Bt4	43.2	25.7	1.3	0.8	1.3	0.9	2.9
	E	53.7	14.9	2.0	0.9	1.0	1.2	6.1
III	Bt2	55.4	14.9	1.0	1.1	1.4	1.0	6.3
	2Bt1	53.1	18.0	1.6	1.0	1.3	1.1	5.0
	A	60.6	24.8	1.5	1.0	1.0	1.3	4.2
IV	E	58.2	21.9	1.4	1.0	1.2	1.1	4.5
	Bt2	52.0	20.6	1.1	1.7	1.8	0.6	4.3
A-5	13.2-13.7	59.7	22.3	1.6	2.2	2.0	0.9	4.5
A-6	20.6-21.0	55.6	17.5	1.2	1.7	1.9	0.6	5.3
A-9s	23.6-24.0	60.1	17.6	1.3	1.7	2.6	0.7	5.8
A-9d	29.6-30.0	54.4	21.9	1.0	1.2	1.7	0.7	4.2
A-14	11.6-12.0	52.4	17.4	1.4	1.7	2.0	0.6	5.1
A-16	27.0-27.5	49.4	19.3	0.9	1.1	1.4	0.6	4.3

[a]Molar ratio.

ORNL/TM-9361

APPENDIX C

DESCRIPTION OF GRAVEL FRACTIONS

APPENDIX C

DESCRIPTION OF GRAVEL FRACTIONS

PROFILE I

A Horizon (0-15 cm)

Color and size: Light to dusky brown; 2-20 mm
Dominant chert type: Altered, stained oolitic
Other chert types: Porous; trace massive
Quartz grains: Frosted; authigenic clusters
Fe-Mn nodules: Few ocherous; not well oxidized
Magnetic fraction: Some large grains
Miscellaneous: Minor sandstone and siltstone

AB Horizon (15-30 cm)

Color and size: Orange-pink to brown; 2-18 mm
Dominant chert type: Altered, stained massive and oolitic
Quartz grains: Frosted to almost clear
Fe-Mn nodules: Ocherous, more oxidized than sample above
Magnetic fraction: Some large grains
Miscellaneous: More heterogeneous than horizon above

BA Horizon (30-46 cm)

Color and size: Light to dusky brown; 2-13 mm
Dominant chert type: Altered, stained massive and oolitic
Quartz grains: Trace frosted
Fe-Mn nodules: Moderately well oxidized
Magnetic fraction: Some large grains
Miscellaneous:

Bt1 Horizon (46-61 cm)

Color and size: White to dusky brown; 2-20 mm
Dominant chert type: Badly altered, stained oolitic and porous
Other chert types: Minor massive
Quartz grains: Minor, frosted
Fe-Mn nodules: Moderately well oxidized
Miscellaneous: Distinctly different appearance from samples above

Bt2 Horizon (62-92 cm)

Color and size: Orange to moderate brown; 2-17 mm
Dominant chert type: Altered, stained massive
Other chert types: Stained, altered, oolitic
Quartz grains: None observed
Fe-Mn nodules: Ocherous
Magnetic fraction: None observed
Miscellaneous: Angular grains, one siltstone chip

APPENDIX C (continued)

PROFILE I (continued)

2Bt3 Horizon (92-120 cm)

Color and size: White to light brown; 2-20 mm
Dominant chert type: Altered, slightly stained massive
Other chert types: Trace, slightly altered and stained oolitic
Quartz grains: Trace, frosted
Fe-Mn nodules: Minor; moderately well oxidized
Magnetic fraction: Very few grains
Miscellaneous: Possibly a few altered siltstone chips

APPENDIX C (continued)

PROFILE II

A Horizon (0-15 cm)

Color and size: Pale orange to yellowish brown; 2-25 mm
Dominant chert type: Altered, stained oolitic
Other chert types: Minor stained massive
Quartz grains: Nil
Fe-Mn nodules: Minor; ocherous; mostly poorly oxidized
Magnetic fraction: Some large grains
Miscellaneous: Chert coarse; fines mostly chert and Fe-Mn oxides

AB Horizon (15-32 cm)

Color and size: Pale orange to dusky brown; 2-12 mm
Dominant chert type: Altered, stained massive and oolitic
Other chert types: Nil
Quartz grains: Trace frosted to clear
Fe-Mn nodules: Yes
Magnetic fraction: Yes
Miscellaneous: A few siltstone chips

Bt1 Horizon (32-58 cm)

Color and size: Pale orange to moderate brown; 2-25 mm
Dominant chert type: Altered, stained massive
Other chert types: Altered, stained oolitic and porous
Quartz grains: Clear to frosted; slightly stained; some authigenic
Fe-Mn nodules: Minor; ocherous; well oxidized
Magnetic fraction: Yes
Miscellaneous: Few altered sandstone chips

Bt2 Horizon (58 to 80 cm)

Color and size: White to dusky brown; 2-16 mm
Dominant chert type: Altered, stained massive and oolitic
Other chert types: Minor porous
Quartz grains: Trace; very fine grained
Fe-Mn nodules: Minor; ocherous; well oxidized
Magnetic fraction: Yes
Miscellaneous: No sand and siltstones

2Bt3 (80-110 cm)

Color and size: Pale orange to dusky brown; 2-7 mm
Dominant chert type: Altered, stained massive
Other chert types: Altered, stained oolitic
Quartz grains: Few authigenic clusters
Fe-Mn nodules: Minor; ocherous; moderately well oxidized
Magnetic fraction: Yes; some large grains
Miscellaneous: Few altered grains; small grains

APPENDIX C (continued)

PROFILE III

E Horizon (0-15 cm)

Color and size: White to brownish black; 2-28 mm
Dominant chert type: Altered, slightly stained massive
Other chert types: Minor altered, stained oolitic, porous, and banded
Quartz grains: Very fine, frosted to nearly clear
Fe-Mn nodules: Trace; small grains; poorly oxidized
Magnetic fraction: Trace
Miscellaneous: Angular grains; some altered sandstone and siltstone

Bt1 Horizon (15-39 cm)

Color and size: White to dusky brown; 2-40 cm
Dominant chert type: Altered, stained massive
Other chert types: Trace altered oolitic and porous
Quartz grains: Trace frosted; trace authigenic
Fe-Mn nodules: Trace; mostly as stains; poorly oxidized
Magnetic fraction: Minor
Miscellaneous: Relatively angular; very large grains

Bt2 Horizon (39-60 cm)

Color and size: White to dusky brown; 2-40 mm
Dominant chert type: Altered, slightly stained massive
Other chert types: Patchy areas banded; oolitic; porous
Quartz grains: Very fine, frosted; authigenic
Fe-Mn nodules: Minor, mostly as stains; more than samples above
Magnetic fraction: Trace
Miscellaneous: Trace dolomoldic chert present

2Btx/Ex Horizon (60-115 cm)

Color and size: White to dusky brown; 2-27 mm
Dominant chert type: Altered, slightly stained massive
Other chert types: Trace oolitic; banded; dolomoldic
Quartz grains: Very fine, frosted to nearly clear; some authigenic
Fe-Mn nodules: Minor, mostly as stains; moderately oxidized
Magnetic fraction: Minor
Miscellaneous: Chert matrix sandstone present

2Bt1 Horizon (115 to 150 cm)

Color and size: Nearly white to dusky brown; 2-35 mm
Dominant chert type: Altered, slightly stained massive
Other chert types: Minor oolitic; porous
Quartz grains: Trace, frosted; authigenic
Fe-Mn nodules: Trace, mostly as stains; moderately oxidized
Magnetic fraction: Trace
Miscellaneous: Chert matrix sandstone present

APPENDIX C (continued)

Profile IV

A Horizon (0-15 cm)

Color and size: Pale orange to yellowish brown; 2-35 mm
Dominant chert type: Altered and stained, massive
Other chert types: Dolomoldic; minor oolitic
Quartz grains: Frosted to nearly clear; some authigenic
Fe-Mn nodules: Dark stains; few isolated grains; poorly oxidized
Magnetic fraction: Trace
Miscellaneous: Some severely altered, blocky sandstone chips

E, EB, BE Horizons (15-55 cm)

Color and size: Light gray to grayish orange; 2-40 mm
Dominant chert type: Mostly massive; porous and/or dolomoldic
Other chert types: Nil
Quartz grains: Trace frosted; some authigenic
Fe-Mn nodules: Nil, minor surface stains; moderately oxidized
Magnetic fraction: Yes, trace
Miscellaneous: Relatively fresh material; few siltstone fragments

Bt1 Horizon (55-80 cm)

Color and size: Pale orange to light brown; 2-45 mm
Dominant chert type: Altered, massive; pitted surfaces, dolomoldic
Other chert types: Nil
Quartz grains: Few frosted to clear grains
Fe-Mn nodules: Nil; ocherous in rinds; well oxidized
Magnetic fraction: Nil
Miscellaneous: Distinctive physical appearance of cherts

Bt2 Horizon (80-150 cm)

Color and size: Pale orange to light brown; 2-25 mm
Dominant chert type: Badly decomposed, very porous, dolomoldic
Other chert types: Nil
Quartz grains: Many well-rounded grains, frosted and clear
Fe-Mn nodules: Nil; ocherous in rinds; well oxidized
Magnetic fraction: Nil
Miscellaneous: Clean but decomposed; high proportion of sand grains

Bt3 Horizon (150-175 cm)

Color and size: Light gray to light brown; 2-37 mm
Dominant chert type: Relatively fresh, massive, porous, and dolomoldic
Other chert types: Banded
Quartz grains: 50% of fines consist of rounded, frosted grains
Fe-Mn nodules: Nil; mostly as ocherous stains; well oxidized
Magnetic fraction: Trace
Miscellaneous: Some very angular, dolomoldic forms present

APPENDIX C (continued)

PROFILE V

E1 Horizon (0-15 cm)

Color and size: Pale orange to dusky brown; 2-25 cm
Dominant chert type: Mostly massive, altered and stained
Other chert types: Dolomoldic
Quartz grains: Minor frosted to clear
Fe-Mn nodules: Mostly as stains/replacements; poorly oxidized
Magnetic fraction: Trace
Miscellaneous: Relatively angular grains

E/Bt Horizon (15-38 cm)

Color and size: Nearly white to grayish brown; 2-18 mm
Dominant chert type: Altered and stained, massive, slightly porous
Other chert types: Oolitic
Quartz grains: Trace, frosted and clear
Fe-Mn nodules: Mostly as stains, but a few large, oxidized grains
Magnetic fraction: Yes; minor; one large grain
Miscellaneous: More oxidized than layer above

Bt/E Horizon (38-55 cm)

Color and size: Light gray to dusky red; 2-22 mm
Dominant chert type: Altered, stained, massive
Other chert types: Some oolitic; trace dolomoldic and banded
Quartz grains: Relatively fresh, mostly frosted, some authigenic
Fe-Mn nodules: Mostly as stains; few large, oxidized grains
Magnetic fraction: Yes, minor
Miscellaneous: Relatively well oxidized; similar to layer above

Bt1 Horizon (55-95 cm)

No gravel fraction

Bt2 Horizon (95-150 cm)

Color and size: Light gray to light brown; 2-30 mm
Dominant chert type: Massive to banded; pitted and stained surfaces
Other chert types: Nil
Quartz grains: Nil; minor authigenic areas in cherts
Fe-Mn nodules: Nil; stains on some surfaces; relatively well oxidized
Magnetic fraction: Nil
Miscellaneous: Relatively fresh; generally angular grains

APPENDIX C (continued)

RESIDUUM

A-5 Core Sample (13.2-13.7 m)

Color and size: Light gray to light bluish gray; slightly stained pale yellowish orange; 2-5 mm
Chert types: Massive to slightly porous; finely crystalline
Quartz grains: None observed
Fe-Mn nodules: None observed
Magnetic fraction: None
Miscellaneous: Some drusy crystals on chert surfaces; very small sample

A-6 Core Sample (20.6-21.0 m)

Color and size: Mostly light gray, but many grains stained with Fe-Mn oxides range from various shades of orange and brown to nearly black; 2-25 mm
Chert types: Mostly massive; some finely crystalline, dolomoldic. porous and oolitic
Quartz grains: Trace; clear to slightly frosted
Fe-Mn nodules: Mostly as stains; some grains
Magnetic fraction: A few magnetic grains present
Miscellaneous: Some of the severely altered oolitic cherts appear to be releasing unaltered grains of quartz.

A-9s Core Sample (23.6-24.0 m)

Color and size: Mostly light to medium gray, slightly stained; 2-18 mm
Chert types: Mostly massive; a few are banded or slightly porous
Quartz grains: Nil
Fe-Mn nodules: A few isolated grains observed
Magnetic fraction: None observed
Miscellaneous: Chert relatively unaltered; some drusy quartz grains on surface

A-9d Core Sample (29.6-30.0 m)

Color and size: Wide range of colors from shades of gray and orange to nearly black; 2-23 mm
Chert types: Very heterogeneous; massive, oolitic, banded; drusy, porous
Quartz grains: Some authigenic quartz clusters present
Fe-Mn nodules: Mostly as stains and coatings
Magnetic fraction: None observed
Miscellaneous: Some material appears fresh while other grains appear altered.

APPENDIX C (continued)

RESIDUUM (continued)

A-14 Core Sample (11.6-12.0 m)

Color and size: Nearly black; 2-9 mm (see note below)
Chert types: Nil
Quartz grains: Nil
Fe-Mn nodules: A few grains observed
Magnetic fraction: None observed
Miscellaneous: Most of the sample disintegrated when washed. Only three small Fe-Mn oxide grains, which contain traces of quartz and chert, remain.

A-16 Core Sample (27.0-27.5 m)

Color and size: Nearly white to gray, slightly stained; 2-17 mm (see miscellaneous below)
Chert types: Massive, slightly banded and oolitic
Fe-Mn nodules: Mostly as stain on chert grains
Magnetic fraction: None observed
Miscellaneous: Two of the smaller grains appear to be chips of siltstone. Most of the material disintegrated when the sample was washed.

APPENDIX D

DESCRIPTION OF SAND FRACTIONS

APPENDIX D

DESCRIPTION OF SAND FRACTIONS

Profile I

A Horizon (0-15 cm)

Color(s): Pale orange-gray to moderate brown
Quartz grains: Mostly frosted, few clear; rounded to angular
Fe-Mn nodules: Mostly large, rounded, altered, many are magnetic
Other phases: Most chert in sand sizes; some angular, stained
Miscellaneous: Chert is relatively coarse

BtlHorizon (46-69 cm

Color(s): Mostly light to moderate brown; few lighter and darker
Quartz grains: Mostly <1 mm; rounded to subangular; frosted to clear
Fe-Mn nodules: Most relatively coarse; varied shapes, altered; some are magnetic
Other phases: Various chert types and sizes; alteration present
Miscellaneous: Some ferruginous sandstone/siltstone chips present

2Bt3 Horizon (92-120 cm)

Color(s): Mostly light brown; some white, pale orange, brown to dusky brown
Quartz grains: Frosted to relatively clear; rounded to angular; some authigenic
Fe-Mn nodules: Coarse to fine size; fresh to altered; 10% are magnetic
Other phases: Coarse to fine size; fresh to altered; massive, oolitic chert
Miscellaneous: More large chert gains than most samples

APPENDIX D (continued)

Profile II

A Horizon (0-15 cm)

Color(s): Mostly light brown; larger grains mostly moderate brown
Quartz grains: Mostly <1 mm; frosted to clear; subrounded to subangular
Fe-Mn nodules: Oxidized, rounded grains, various sizes; minor magnetic
Other phases: Altered, stained, massive chert; minor oolitic, porous
Miscellaneous: One of the magnetic crystals appears to have developed faces.

Bt2 Horizon (58-80 cm)

Color(s): Mostly moderate orange-pink; larger grains range up to dusky brown
Quartz grains: Mostly <1 mm; frosted to clear; rounded to subangular
Fe-Mn nodules: Oxidized; various sizes and shapes; minor magnetic
Other phases: Mostly stained, massive, oolitic chert; severely altered
Miscellaneous: Larger Fe-Mn grains are more magnetic.

2Bt4 Horizon (110-150 cm)

Color(s): Mostly very pale orange to moderate orange-pink
Quartz grains: Mostly <1 mm; relatively clear; finer grains more frosted, rounded
Fe-Mn nodules: Larger grains relatively fresh; the rest well oxidized
Other phases: Some large grains, relatively stained; massive, oolitic chert
Miscellaneous: Some authigenic quartz grains present

APPENDIX D (continued)

PROFILE III

E Horizon (0-15 cm)

Color(s): Pale orange to shades of brown
Quartz grains: Mostly <1 mm; frosted to clear; rounded to subangular
Fe-Mn nodules: Few grains; alteration; replacements; minor magnetic
Other phases: Variety of chert types; fresh to severely altered
Miscellaneous: Some authigenic quartz grains present

Bt2 Horizon (39-60 cm)

Color(s): Pale orange to grayish orange; few white to shades of brown
Quartz grains: Mostly <1 mm; rounded to subrounded; mostly frosted
Fe-Mn nodules: Fresh to altered; some replacements; minor magnetic
Other phases: Various chert types; oolitic, massive, porous, fresh to altered
Miscellaneous: Some authigenic quartz present

2Bt1 Horizon (115-150 cm)

Color(s): Mostly pale orange; some white to shades of brown
Quartz grains: Mostly <1 mm; rounded to subangular; frosted, few clear
Fe-Mn oxides: Oxidized and ocherous; few fresh grains; minor magnetic
Other phases: Various chert types; massive, oolitic, dolomoldic; some altered
Miscellaneous: Some authigenic quartz present

APPENDIX D (continued)

Profile IV

A Horizon (0-15 cm)

Color(s): Pale orange to moderate to dusky brown
Quartz grains: Subangular, some rounded; some authigenic
Fe-Mn nodules: Various sizes and shapes, alteration; trace is magnetic
Other phases: Most chert is large, altered; dolomoldic, porous
Miscellaneous:

E Horizon (15-48 cm)

Color(s): Moderate orange-pink to light brown; few dusky brown
Quartz grains: Mostly <1 mm; frosted to clear; various sizes and shapes
Fe-Mn oxides: Severely altered; stained and irregular shapes; minor magnetic
Other phases: Severely altered, stained, large, massive dolomoldic chert
Miscellaneous: Relatively large amount of chert present

Bt2 Horizon (80-150 cm)

Color(s): Grayish orange to pale yellowish orange; some white
Quartz grains: Dominant phase; frosted, well rounded
Fe-Mn nodules: Nil; few ocherous grains
Other phases: Largest grains present; mostly dolomoldic, massive chert
Miscellaneous: Most quartz-rich sample; best-rounded grains

APPENDIX D (continued)

Residuum

A-5 Core Sample (13.2-13.7 cm)

No sand fraction

A-6 Core Sample (20.6-21.0 m)

Color(s): Pale orange to grayish orange; some dark grains
Quartz grains: Mostly <1 mm; round, clear to milky, frosted, angular
Fe-Mn nodules: Varied; small grains; stained chert, 20-25% magnetic
Other phases: Coarse, angular cherts; fine, angular milky chert
Miscellaneous: Relatively fresh to deeply weathered grains; several chert types

A-9s Core Sample (23.6-24.0 m)

Color(s): Variable; grayish orange to dusky brown
Quartz grains: Mostly clear, authigenic; some rounded; frosted grains
Fe-Mn nodules: Much Fe-Mn material, 25%; mostly not magnetic
Other phases: Coarse, angular, milky; fine, silt-sized, angular chert
Miscellaneous: Amount of quartz relatively small, 5-10%

A-9d Core Sample (29.6-30.0 m)

Color(s): Mostly yellowish brown; few almost white; moderate to dusky brown
Quartz grains: Fine grains, stained; few large grains and clusters
Fe-Mn nodules: 10% fine to coarse grains; irregular shapes
Other phases: Mostly coarse, irregular chert; lesser amount of fine grains
Miscellaneous: Coarse chert relatively fresh; some oolitic grains

A-14 Core Sample (11.6-12.0 m)

Color(s): Mostly variable pale orange; few black nodules
Quartz grains: Mostly frosted, subrounded; frosted, silt-sized, angular
Fe-Mn nodules: Nodular, black, irregular grains; mostly nonmagnetic
Other phases: Mostly fine, white, irregular; few larger chips
Miscellaneous: Mostly relatively fresh; few altered Fe-Mn oxides

A-16 Core Sample (27.0-27.5 m)

Color(s): Mostly pale orange to yellowish brown; very few dark grains
Quartz grains: Wide range of sizes; clear to frosted; rounded to angular
Fe-Mn nodules: Mostly <1 mm; fresh to severely altered; mostly nonmagnetic
Other phases: Mostly fine; angular, altered; few 1-mm, irregular grains
Miscellaneous: Relatively clean sample

ORNL/TM-9361

INTERNAL DISTRIBUTION

1. S. I. Auerbach
2-11. L. D. Bates
12. W. J. Boegly, Jr.
13. R. O. Chester
14. R. B. Clapp
15. J. H. Coobs
16. N. H. Cutshall
17. E. C. Davis
18. L. R. Dole
19. L. D. Eyman
20. C. S. Haase
21. S. G. Hildebrand
22. D. D. Huff
23. A. D. Kelmers
24. R. H. Ketelle
25. D. W. Lee
26-30. S. Y. Lee
31. T. F. Lomenick
32. L. J. Mezga
33. T. W. Oakes
34. C. R. Olsen
35. D. E. Reichle
36. T. H. Row
37. F. G. Seeley
38. E. D. Smith
39. B. P. Spalding
40. S. H. Stow
41-50. L. E. Stratton
51. J. Switek
52. T. Tamura
53. H. Zittel
54. Central Research Library
55-70. ESD Library
71-72. Laboratory Records Dept.
73. Laboratory Records, ORNL-RC
74. ORNL Patent Section
75. ORNL Y-12 Technical Library

EXTERNAL DISTRIBUTION

76. J. F. Albaugh, Program Manager, Solid Waste Processing and Disposal, Rockwell Hanford Operations, P.O. Box 800, Richland, WA 99352
77. E. L. Albenesius, Savannah River Laboratory, P.O. Box A, Aiken, SC 29801
78. M. Barainca, Program Manager, Low-Level Waste Management Program, U.S. Department of Energy, 550 Second Street, Idaho Falls, ID 83401
79. D. R. Brown, Manager, ORO Radioactive Waste Management Program, U.S. Department of Energy, Oak Ridge Operations, P.O. Box E, Oak Ridge, TN 37831
80. T. C. Chee, R&D and Byproducts Division, DP-123 (GTN), U.S. Department of Energy, Washington, DC 20545
81. Peter Colombo, Group Leader, Nuclear Waste Research, Brookhaven National Laboratory, Bldg. 701, Upton, NY 11973
82. E. F. Conti, Office of Nuclear Regulatory Research, Nuclear Regulatory Commission, MS-1130-SS, Washington, DC 20555
83. J. J. Davis, Office of Nuclear Regulatory Research, Nuclear Regulatory Commission, MS-1130-SS, Washington, DC 20555
84. J. E. Dieckhoner, Acting Director, Operations and Traffic Division, DP-122 (GTN), U S. Department of Energy, Washington, DC 20545
85. Carl Gertz, Director, Radioactive Waste Technology Division, Idaho Operations Office, U.S. Department of Energy, 550 Second Street, Idaho Falls, ID 83401

86. E. A. Jennrich, Program Manager, Low-Level Waste Management Program, EG&G Idaho, Inc., P.O. Box 1625, Idaho Falls, ID 83415
87. J. J. Jicha, Director, R&D and Byproducts Division, DP-123 (GTN), U.S. Department of Energy, Washington, DC 20545
88. E. A. Jordan, NE-25 (GTN), U.S. Department of Energy, Washington, DC 20545
89. P. W. Kaspar, Assistant Manager for Safety and Environment, U.S. Department of Energy, Oak Ridge Operations, P.O. Box E, Oak Ridge, TN 37831
90. J. Howard Kittel, Manager, Office of Waste Management Programs, Argonne National Laboratory, 9700 S. Cass Ave., Bldg. 205, Argonne, IL 60439
91-95. O. C. Kopp, Department of Geological Science, University of Tennessee, Knoxville, TN 37916
96. M. R. Kreiter, Waste Isolation, Pacific Northwest Laboratory, Richland, WA 99352
97. Leonard Lane, Los Alamos National Laboratory, P.O. Box 1663, Los Alamos, NM 87545
98. D. E. Large, National Program Manager, ORO Radioactive Waste Management Program, Oak Ridge Operations Office, U.S. Department of Energy, P.O. Box E, Oak Ridge, TN 37831
99. D. B. Leclaire, Director, Office of Defense Waste and Byproducts Management, DP-12 (GTN), U.S. Department of Energy, Washington, DC 20545
100-101. J. A. Lenhard, Oak Ridge Operations, P.O. Box E, U.S. Department of Energy, Oak Ridge, TN 37831
102-106. D. A. Lietzke, Department of Plant and Soil Science, University of Tennessee, Knoxville, TN 37916
107. Helen McCammon, Director, Ecological Research Division, Office of Health and Environmental Research, Office of Energy Research, MS-E201, ER-75, Room E-233, U.S. Department of Energy, Washington, DC 20545
108. G. L. Meyer, Environmental Protection Agency, 401 M Street SW, MS-ANR459, Washington, DC 20460
109. Harold A. Mooney, Department of Biological Sciences, Stanford University, Stanford, CA 94305
110. Donald T. Oakley, Program Manager for Waste Management, Los Alamos National Laboratory, P.O. Box 1663, Los Alamos, NM 87545
111. Edward O'Donnell, Division of Radiation Programs and Earth Sciences, U.S. Nuclear Regulatory Commission, Mail Stop 1130 SS, Washington, DC 20555
112. William S. Osburn, Jr., Ecological Research Division, Office of Health and Environmental Research, Office of Energy Research, MS-E201, EV-33, Room F-216, U.S. Department of Energy, Washington, DC 20545
113. J. W. Patterson, Program Director, Waste Management Program Office, Rockwell Hanford Operations, P.O. Box 800, Richland, WA 99352

114. Irwin Remson, Department of Applied Earth Sciences, Stanford University, Stanford, CA 94305
115. Paul G. Risser, Office of the Chief, Illinois Natural History Survey, Natural Resources Building, 607 E. Peabody Ave., Champaign, IL 61820
116. Jackson Robertson, USGS, 410 National Center, Reston, VA 22092
117. E. M. Romney, University of California, Los Angeles, 900 Veteran Avenue, Los Angeles, CA 90024
118. E. R. Rothschild, CH_2M Hill, 310 W Wisconsin Ave., P.O. Box 2090, Milwaukee, WI 53201
119. R. J. Starmer, HLW Technical Development Branch, Office of Nuclear Material Safety and Safeguards, Nuclear Regulatory Commission, Room 427-SS, Washington, DC 20555
120. J. G. Steger, Environmental Sciences Group, Los Alamos Scientific Laboratory, MS-K495, P.O. Box 1663, Los Alamos, NM 87545
121. J. A. Stone, Savannah River Laboratory, E. I. DuPont de Nemours and Company, Bldg. 773-A, Room E-112, Aiken, SC 29808
122. Robert L. Watters, Ecological Research Division, Office of Health and Environmental Research, Office of Energy Research, MS-E201, ER-75, Room F-226, U.S. Department of Energy, Washington, DC 20545
123. Frank J. Wobber, Division of Ecological Research, Office of Health and Environmental Research, Office of Energy Research, MS-E201, U.S. Department of Energy, Washington, DC 20545
124. Robert W. Wood, Director, Division of Pollutant Characterization and Safety Research, U.S. Department of Energy, Washington, DC 20545
125-151. Technical Information Center, Oak Ridge, TN 37831

☆U.S. GOVERNMENT PRINTING OFFICE: 1984-544-045/4237